Model Based ECG Denoising Using Discrete Bionic Wavelet Transform

By

(Md. Abdul Awal)

A thesis submitted in partial fulfillment of the requirement for the degree of
Master of Science in Biomedical Engineering

Khulna University of Engineering & Technology
Khulna 9203, Bangladesh

December 2011

Declaration

This is to certify that the thesis work entitled "**Model Based ECG Denoising Using Discrete Bionic Wavelet Transform**" has been carried out by **Md. Abdul Awal** in the Department of Biomedical Engineering, Khulna University of Engineering & Technology, Khulna, Bangladesh. The above thesis work or any part of this work has not been submitted anywhere for the award of any degree or diploma.

07/12/2011

Signature of Supervisor

Signature of Candidate

Approval

This is to certify that the thesis work submitted by Md. Abdul Awal entitled "Model Based ECG Denoising Using Discrete Bionic Wavelet Transform" has been approved by the board of examiners for the partial fulfillment of the requirements for the degree of M. Sc. Engineering in the Department of Biomedical Engineering, Khulna University of Engineering & Technology, Khulna, Bangladesh in December 2011.

BOARD OF EXAMINERS

1. _____ 07/12/2011
   Prof. Dr. Mohiuddin Ahmad
   Dept. of Electrical and Electronic Engineering
   Khulna University of Engineering & Technology
   Khulna-9203, Bangladesh
   — Chairman (Supervisor)

2. _____ 07/12/2011
   Head of the Department
   Dept. of Biomedical Engineering
   Khulna University of Engineering & Technology
   Khulna-9203, Bangladesh
   — Member

3. _____ 07.12.11
   Dr. Md. Shahjahan
   Associate Professor
   Dept. of Electrical and Electronic Engineering
   Khulna University of Engineering & Technology
   Khulna-9203, Bangladesh
   — Member

4. _____
   Dr. Mohammad Shaifur Rahman
   Associate Professor
   Dept. of Electrical and Electronic Engineering
   Khulna University of Engineering & Technology
   Khulna-9203, Bangladesh
   — Member

5. _____ 07/12/2011
   Prof. Dr. Md. Al-Amin Bhuiyan
   Dept. of Computer Science & Engineering
   Jahangirnagar University
   Savar, Dhaka-1342, Bangladesh
   — Member (External)

ACKNOWLEDGEMENTS

First of all, I acknowledge my gratitude and thanks to almighty ALLAH for successful completion of my thesis.

I am indeed fortunate to have work under the guidance of Prof. Dr. Mohiuddin Ahmad. His contagious suggestions, encouragement, patience, originality and desired to succeed have helped me complete into this thesis. His proper guidelines, inspiration and helpful contribution in the research work and spent-time played a vital role in completion this thesis work. Dr. Mohiuddin Ahmad is an intellectual in signal processing, time-frequency analysis and soft computing. He is the source of vast ideas, profound knowledge and feedback all the time for authors. For all of these, the author gratefully acknowledges his advices and guidelines from the deep corner of heart.

I also acknowledge my deep gratitude to Prof. Dr. Md. Al-Amin Bhuiyan for his useful suggestions and remarks.

A number of important personalities have shaped me and educational background. My mother, my brother and my sister, encouraged me to keep striving to gain higher education and to set and achieve higher goals all time. I have been very fortunate to have been assisted by Dr. Md. Sohel Mahmud Sher and Dr. Rameswar Debnath of Khulna University in many ways. I also acknowledge my appreciation to my friend Saiful Islam Sunny, who helped me by giving valuable papers from different journals. I am also grateful to Sheikh Shanawaz Mostafa for his continuous support and encouragement.

Furthermore, I would like to thank all the faculty members of Electrical and Electronic Engineering Department and Biomedical Engineering Department, KUET, my all colleagues of Khulna University and my well wishers for helping in various ways in formulating this dissertation.

Abstract

Electrocardiogram (ECG) is a measurement of bio-electric potential produced by rhythmical cardiac activities, contraction and relaxation of the cardiac muscle produced at sinoatrial (SA) node. This electric potential associated with the cardiac cycle can be detected at the surface of the body, amplified and recorded as a time record of each cardiac cycle. Different cardiac function such as heart rate, abnormality of rhythm can easily be identified by ECG and it is a low cost tools in the medical diagnostic system. Therefore, ECG signal modeling and processing is one of the most significant topic in biomedical signal analysis.

Most of the ECG models are complex and their computational time is high. In this research, a Gaussian wave-based model is proposed which can simulate ECG wave as well as its P, Q, R, S and T components individually. In addition, dynamically shifting baseline of the model reduces the preprocessing of ECG signal. The coefficient of the model is calculated by nonlinear least square technique using Gauss-Newton algorithm. The model fits well with real ECG by Normalized Root Mean Square error (NRMSE) of 0.0034 at the normal condition. Further analyses have been performed to evaluate the models ability of representing the different cardiac Dysrhythmias like atrial fibrillation, brachycardia and tachycardia successfully. For better model fitting denoised ECG plays a significant role.

Bionic wavelet Transform (BWT) is based on auditory model but it is not efficient for ECG signal processing since ECG is generated from the heart. So for denoising ECG, a new adaptive wavelet transform is developed based on heart- arterial interaction model. Adaptability is adjusted instantaneous amplitude of the signal and its first-order difference. The automatically adjusted resolution is achieved by introducing the active control mechanism of the cardiac system into the wavelet transform. It is very hard to know what entropy function used in the bio-system. This is the problems of other transforms. But, the discrete BWT uses active control mechanism in the cardiac system to adjust the wavelet function rather than entropy function as criterion. Moreover, due to various oscillating behavior of different types of ECG signal constant Quality factor (Q) of wavelet is not as effective as variable Q. The variable Q is changed with the instantaneous value of a signal and it will make BWT more adaptive compared to Tunable Q wavelet transform (TQWT). As in variable Q-wavelet transform like DBWT

which is the discrete version of BWT, Q is changed with the instantaneous value of a signal and its first order difference instead of Q-factor is tuned to a fixed value in TQWT. In addition, our proposed modified S-median thresholding technique has an adjustable factor and introduced in the system for better performance. In order to compare DBWT with other wavelet transform, experiments on traditional WT, multi-adaptive BWT, TQWT were conducted on both constructed signals and real ECG signals. The results show that novel DBWT performs better than these three wavelet transforms, and is appropriate for cardiac signal processing, especially over noisy environment.

Contents

LIST OF TABLES

LIST OF FIGURES

List of Abbreviation

AV	Atrio-Ventricular
BWT	Bionic Wavelet Transform
BW	Baseline Wander
ChAD	Chip Away Decomposition
DFT	Discrete Fourier Transform
DBWT	Discrete Bionic Wavelet Transform
DWT	Discrete Wavelet Transform
ECG	Electrocardiogram
EMG	Electromyogram
EM	Electrode Movement
FT	Fourier transform
LMS	Least Mean Square
MA	Muscle Artifact
MSE	Mean Square Error
MSC	Magnitude Squared Coherence
MIT-BIH	Massachusetts Institute of Technology-Beth Israel Hospital
MABWT	Multiadaptive Bionic Wavelet Transform
NMSE	Normalized Mean Square Error
NRMSE	Normalized Root Mean Square Error
PSD	Power Spectral Density
PRD	Percent Root Mean Difference
RMSE	Root Mean Square Error
SA	Sino-Atrial
STFT	Short-Time Fourier Transform
SURE	Stein Unbiased Risk Estimation
SNR	Signal-to-Noise Ratio
TQWT	Tunable-Q Wavelet Transform
TFR	Time- Frequency representation

Nomenclature

$\psi_{a,\tau}(t)=\frac{1}{\sqrt{a}}\psi(\frac{t-\tau}{a})$, wavelet function where τ and (a >0) represent the time shift and scale variable respectively.

$h(n)$ =low pass filter coefficient.

$g(n)$ =high pass filter coefficient.

ρ = Blood density.

C_o = Pulse wave velocity.

σ = Poisson ratio for arterial wall .

F_{10} = The expression $\frac{2J_1(\alpha j^{3/2})}{\alpha j^{3/2} J_0(\alpha j^{3/2})}$, where J_o and J_1 are Bessel functions of the first kind, and order zero and one, respectively, and Womersley number $\alpha = R_0\sqrt{\omega\rho/\mu}$.

γ = Propagation constant .

ω = Angular frequency.

E = Young's modulus of arterial wall .

h = Wall thickness .

R_o = Internal radius of arterial segment .

η_w = visco-elasticity of the arterial wall.

Γ = reflection coefficient .

μ = blood viscosity.

CHAPTER I

INTRODUCTION

1.1 Electrocardiography

The heart is one of the major organs of the human body, vital to our survival. It is basically a large pump, whose sole purpose is to maintain blood circulation and keep organ alive. This mechanical event is performed by the electrical activity of the heart. Without electrical event mechanical event, i.e. blood circulation, is not possible. These electrical events are investigated by Electrocardiogram (ECG) which is one of the most useful, easily available and low cost tools for the early diagnosis and evaluation of many cardiac problems. But this ECG signal which is non-stationary in nature can potentially be corrupted by various types of noises and artifacts like electrode pop or contact noise, motion artifacts, electromyographic noise, baseline drift, etc. [1] that undergoes incorrect diagnosis and may cause cardiac death. This leads a huge scope to model, remove noise and artifact, compression, feature extraction of this biomedical signal. So the study of such non-stationary signal is very necessary to prevent misdiagnosis (which can lead abnormal morphological change in the ECG cardiac cycle, such as if the P wave get broaden or notch look this will indicate a delay in the depolarization of the left atrium which can create problems in the conduction system. Tall P wave indicates right atrial enlargement. Abnormally large Q wave indicates Myocardial Infarction. Irregular T wave indicates myocardial ischemia, infraction, ventricular hypertrophy, bundle branch block etc. During open-heart surgery polyvinyl chloride (PVC) tubing (or possibly other plastic parts) in the pump can generate electricity through piezoelectric or static electricity effects. This artifact looks somewhat like QRS or pacemaker spikes and hence creates misdiagnosis.

1.2 State of The Art

The establishment of the clinical electrocardiograph (ECG) by the Dutch physician Willem Einthoven in 1903 marked the beginning of a new era in medical diagnostic techniques, including the entry of electronics into health care. Since then, electronics, and subsequently computers, have become integral components of biomedical signal analysis

systems, performing a variety of tasks from data acquisition and processing for removal of artifacts to feature extraction and interpretation.

Though there is an ideal value of PQRST of the ECG signal, but in most of the cases the captured ECG waveforms are different from the ideal one which may complicate in the subsequent analysis of the ECG, because it varies from man to man. The morphological change occurs due to drug, age, gender, preexisting condition, gender/family history, activity etc [1].

Recently, the time- frequency representation (TFR) has been extensively used for the analysis of such non-stationary signal since TFR can obtain the frequency information and its variation along the time simultaneously. In addition, introduction of some biological functions or model parameters in the TFR are also necessary and that makes TFR novel one. Such novel adaptive wavelet transform called Discrete Bionic Wavelet Transform (DBWT) based on the biological active heart-arterial interaction model which is very much compatible with the biomedical signal like ECG signal processing. Moreover, no other transforms are based on the biological model. So bio-system based DBWT is appropriate for bio-signal processing. The unique feature of the BWT is that its resolution in the time-frequency domain can be adaptively adjusted by the signal instantaneous amplitude and its first order differential. Furthermore, it is very hard to know what entropy function used in the bio-system. This is the problems of other transforms. But, the DBWT uses active control mechanism in the cardiac system to adjust the wavelet function rather than entropy function as criterion. Another interesting decisive factor for choosing the DBWT is that, it is a special subset of Adaptive Wavelet Transform (AWT). But the performance of DBWT is highly dependent on the T-function stemming from biological model whereas the performance of AWT is highly dependent on the entropy function. As DBWT is a special division of adaptive transforms and uses biological model. Therefore, DBWT can be a better option for ECG signal processing. Moreover, DBWT can effectively reduce the computational cost and complexity as it is discrete dyadic version of CWT.

A supplementary factor is that, presently, signal-processing strategies are typically based on Band Pass Filters (BPFs), and are implemented using separate hardware and microprocessors. Consequently, with these techniques it is hard to control the signal processing performance because there are too many signal-processing units involved [2] . Recently, K. Nie et al. and C. P. Behrenbech [2] [3] independently experimented with new

signal processing strategies based on wavelet transform (WT) in order to simplify and minimize the hardware, because WT inherently supports all the features of signal processing provided by separate hardware and microprocessors but in fewer units.

One of the common approaches is the adaptive filters architecture which has been used for the noise cancellation of ECGs containing power line interference, baseline wandering, EMG noise and motion artifacts. Other effective techniques such as principle component analysis, independent component analysis, neural networks, Kalman filtering have also been used to extract a noise-free ECG. Over the past several years, with the advances of the ECG signal processing, wavelet transform (WT) method also received a promising result for denoising of signals, feature extraction having multiresolution characteristics.

All the above approaches use traditional linear filters to span the signal in time-frequency domain (WT also can be viewed as a linear BPF bank), and may not be effective for a normal human heart, which analyzes the signal by an active and nonlinear system. Research into the physiology of the human heart shows that the active and nonlinear mechanisms in the heart are necessary for maintaining its high sensitivity and frequency selectivity. The drawbacks with the existing linear signal-processing strategies motivated us to investigate the potential application of DBWT an active and nonlinear method stemming from the active biological model.

Bionic wavelet transforms are comparatively new topics which were first used in the speech signal processing and recently is being used in the biomedical signal processing [4]. As T-function reflects the dynamic control mechanism from the biosystem it is especially suitable for the biological signals. But there is no specified wavelet for cardiac signal. So we proposed a DBWT for cardiac signal processing using heart-interaction model. Moreover, the mathematical model proposed in the thesis is very simple and can be used as a reference model for the future research. An application of our proposed techniques is discussed using support vector machine.

1.3 Objectives

The objectives of this research work are:

- To present the mathematical model of ECG based on the morphology of PQRST of the cardiac cycle.
- To fit the model with the realistic signal collected from the database like MIT-BIH and from the BIOPAC system.
- To denoise and remove different noise from the noisy ECG signals using proposed DBWT and adaptive thresholding (hard, soft and nonlinear) techniques.
- To evaluate the performance of the proposed method and to compare with other techniques.
- To present the quantitative and qualitative evaluation of the transformed signal.
- To demonstrate an application of the proposed techniques using support vector machine.

1.4 Contributions

In this research some useful contributions have been done by the author. Some original outcomes of this research are listed below:

- A simplified mathematical model has been developed which can simulate ECG wave as well as P, Q, R, S and T wave individually. It is capable of simulating various kind of practical phenomena such as brachycardia (slow heart rate), tachycardia (fast heart rate), atrial fibrillation etc.
- A T-function is proposed inspired by human heart-arterial interaction model which was not used before. Discrete Wavelet transform is then adapted by this T-function which is called Discrete bionic wavelet transform. It is very much suitable for ECG signal processing as it is adapted by active biological heart-arterial interaction model. Although DBWT exist, but they used ear model based on otoaccustic emission which is not appropriate specially for ECG signal processing while maintaining the features of Bionic Wavelet transform.
- A modified s-median thresholding method also proposed which has a tuning parameter. The parameter is chosen where SNR improvement posses highest value.

1.4 Application of This Research

In this research a novel wavelet transform named Discrete Bionic Wavelet Transform (DBWT) is proposed. There are many application of this transform in biomedical signal like ECG, EMG, PCG denoising, compression, telemedicine etc. Moreover, the coefficient of the transform can be used to create features for support vector machine, artificial neural network etc. to detect and classify of different diseases.

1.4 Organization of The Thesis

The thesis is organized as follows.

Chapter II: This chapter contains the background knowledge of the ECG signal, its characteristic and origin. Different types of noise and its origin are also discussed here.

Chapter III: In this chapter source of noises in ECG signal are discussed.

Chapter IV: In this chapter we proposed a simplified mathematical model for generating ECG in cardiac dysrhythmias which is fitted by non-linear least square techniques. Goodness of fitting is analyzed for evaluating the performance of the model in both time domain and frequency domain.

Chapter V: In this section a novel wavelet transform is proposed where T-function is stemmed from heart-arterial interaction model. A modified S-median thresholding technique is also introduced for better performance. Performance of the proposed transform with modified thresholding techniques is compared with recent and well known wavelet techniques.

Chapter VI: Finally the thesis concludes with some closing remarks and directions of further research are discussed in this chapter.

CHAPTER II

THE FUNCTION OF HEART AND ECG

2.1 Human Heart

The human heart is a biological pump. It receives blood from veins and pumps the blood into arteries. The heart contains four chambers and several one-way valves as shown in Fig 2.1 a wall or septum divides the heart into left and right sides, in a double pump configuration. Each side is then further divided into an upper chamber called atrium, and a lower chamber called ventricle. The right side of the heart receives de-oxygenated blood from the venous systems which is then pumped to the lungs via the pulmonary loop where the carbon dioxide in the blood is exchanged for oxygen. The left side of the heart receives the oxygenated blood from the lungs and pumps it into the systemic loop for distribution throughout the body. The structure and function of heart are depicted in Fig. 2.1 and Fig. 2.2.

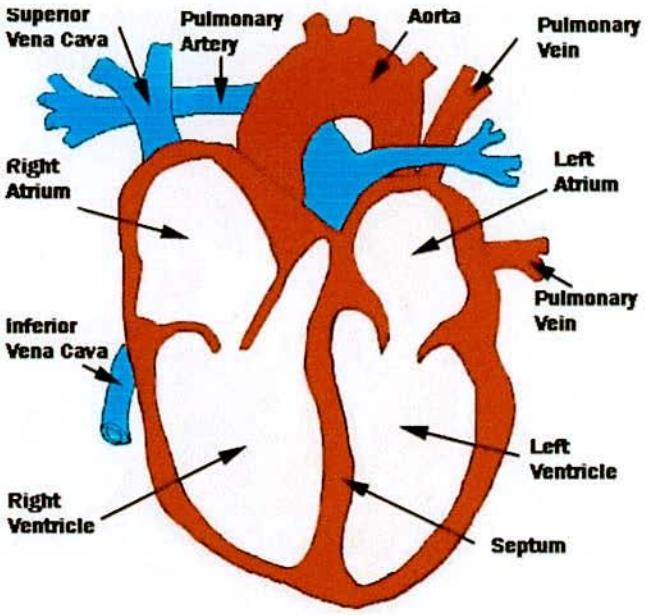

Figure 2.1: Structure of heart

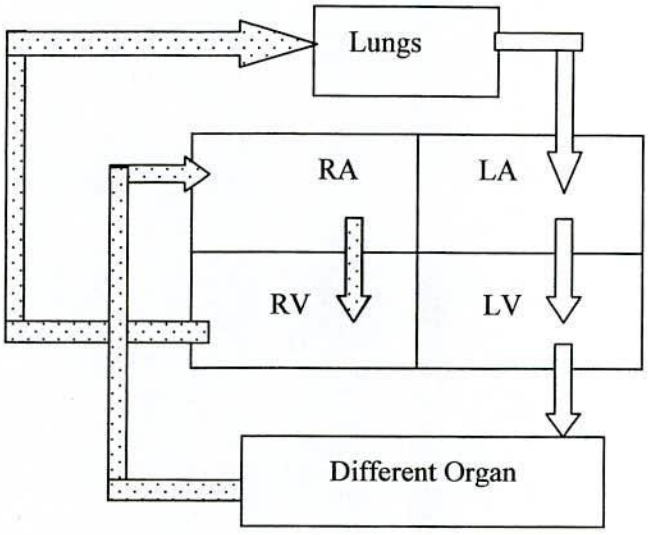

Figure 2.2: Human Heart chambers and blood flow diagram. Where grinded arrow represents the flow of contaminated (CO_2) blood and normal arrow denotes fresh (O_2) blood.

The human heart is *myogenic* (*myo*=muscle, *gene*=origin), that is, the signal for the heart to beat comes from the heart itself and not from an external source such as nerve cell. Although the heart is supplied with motor nerves that can influence either the rate of contraction or strength of contraction, the extrinsic nerves plays no role in the genesis of the heart beat. If the extrinsic nerves (sympathetic and para-sympathetic) were cut, or even if the heart were to be removed from the body, it would continue to beat rhythmically as long as it was supplied with oxygen and vital nutrients, had wastes material removed and its normal temperature maintained. Thus the heart possesses unique ability to initiate and undergo a cardiac muscle or heartbeat by itself without any stimulation from rest of the body. This property of cardiac muscle is called *inherent rhythmicity* or *automaticity*.

2.1.1 Control and Coordination of *Myocardium*

The control and coordination of *myocardium's* (*myo*=muscle, *cardia*=heart) inherent rhythmicity is dependent on a specialized system of conductive tissue within the heart. Before each contraction of the heart, an electric current must first pass through the myocardial fibers. The conduction system of the heart is responsible for generating these electrical currents and conveying them in an orderly fashion to all parts of the heart. The

conduction system consists of the following areas of specialized conducting tissues: Sinoatrial (SA) node, intermodal and interatrial pathways, the atrioventricular (AV) node, the bundle of His, right and left bundle branch.

The contraction of the various muscles of the heart enables the blood to be pumped. While the myocardial muscle cells can contract spontaneously, under normal conditions these contractions are triggered by action potentials originating from pacemaker cells situated in two areas of the heart - the Sino-Atrial (SA) and Atrio-Ventricular (AV) nodes. The SA pacemaker cells can spontaneously generate action potentials at 60-80 times per minute, but are themselves under the control of the sympathetic and parasympathetic nervous system. The SA node generally triggers the action potential for a heartbeat, but the AV node can take over this role if for some reason the SA node fails.

2.1.2 Sequence of Events of Human Heartbeat

The normal cycle of a heartbeat has the following sequence of events :

a) The SA node normally generates an action potential i.e. electrical impulse, which spreads across both atria. The SA node, without neural and endocrine stimulation, spontaneously depolarizes at the rate between 60 to 80 times per minute. It paces the electrical and mechanical events of the entire heart. Therefore, the SA node is called the natural pacemaker.
b) This spreading action potential results in the simultaneous contraction of the left and right atria via interatrial pathways.
c) This action potential is also passed to the AV node via the inter-nodal conducting fibres, which is a part of the Junctional tissue between the right atrium and ventricle.
d) During the contraction of the atria, blood from the atria is pushed to the respective ventricle.
e) The AV node's own action potential is triggered by the action potential arriving from the SA node after a slight delay. The delay allows the atria to contract before excitation of the ventricles occurs. The delay also helps to protect the ventricles from rapid atrial impulses. The AV action potential is spreaded to the ventricles via further conducting fibers, resulting in a delay of about 110msec, which is sufficient

to ensure that the atrial contraction is over.

f) After passing the AV node, the impulse is carried to the ventricles through the bundle of Hiss, a common bundle of specialized conductive fibers lying along the upper part of the interventricular septum. The bundle of Hiss runs down within the upper interventricular septum and branches into a right and left bundle.

g) The right bundle branch carries the impulse to the right ventricle; the left bundle branch carries the impulse to the left ventricle. Each bundle branch further subdivided into numerous small conducting fibers called purkinje fibers, which relay the electric impulse directly to ventriclar muscle, stimulating the ventricle to contract.

h) The action potential triggers both ventricles to contract and push blood into the arterial system. The left ventricle supplies the systemic arterial system while the right ventricle supplies the pulmonary system where the blood is oxygenated by the lungs.

i) All muscles of the heart then relax and blood continues to flow due to the elastic recoil of the arterial walls. During this period both atria and ventricles fill with blood as it returns from the body via the venous system. A series of one- way valves at the input and outputs of the atria and ventricles determine the direction of blood flow.

In summary, the contraction of the cardiac muscle is associated with an electric impulse initiated at the sinuatrial node, which sweeps over the conduction path of the heart, preceding the mechanical change in the muscle. In each normal cardiac cycle, the electrical event follow the sequence : (1) Depolarization and repolarization of the (SA) node; (2) depolarization and repolarization of atrial muscles;(3) Depolarization and repolarization of AV node and bundle;(4) Depolarization and repolarization of purkinje network;(5) Depolarization and repolarization of ventricular muscles. The whole process can be shown in block diagram as Fig. 2.3.

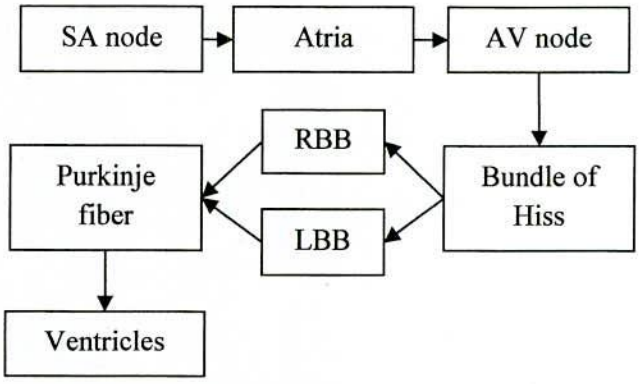

Figure 2.3: Sources of electrical activity in heart.

2.2 Electrocardiography (ECG)

The various propagating action potentials within the heart produce a current flow, which generates an electrical field that can be detected, in significantly attenuated form, at the body surface, via a differential voltage measurement system as a time record of the electrical events occurring during each cardiac cycle. Thus, heart rate can be accurately determined and abnormalities of rhythm and conduction can be identified. The electrical and mechanical device that records the electrical activity of each cardiac cycle is called an electrocardiograph. The study of electrocardiograph's application and its interpretation is called electrocardiography.

So, ECG (or in German EKG) is a graphic representation of the electrical activity of the heart's conduction system recorded over a period of time. Under normal conditions, ECG tracings have a very predictable direction, duration, and amplitude. Because of this, the various components of the ECG tracing can be identified, assessed, and interpreted as to normal or abnormal function. The ECG is also used to monitor the heart's response to the therapeutic interventions. Because the ECG is such a useful tool in the clinical setting, the respiratory care practitioner must have a basic and appropriate understanding of ECG analysis. The electric current associated with and generated during the cardiac cycle is detected by placing a positive electrode and a negative electrode on the selected areas of the skin surface and recording the electric current changes occurring between the electrodes as the heart beats. The particular arrangements of two electrodes, one positive

and the other negative, with respect to a third electrode, the ground electrode is called Lead.

2.2.1 ECG Leads

There are 15 Leads: 3 Standard bipolar limb leads (I, II, III), 6 precordial unipolar chest leads (V_1,V_2,V_3,V_4,V_5,V_6), 3 augmented unipolar limb leads (AVF, AVR,AVL) and 3 bipolar chest leads (CR,CL,CF). The most commonly employed leads are bipolar limb leads and in this research ECE will be investigated by lead II.

2.2.2 Morphology of ECG

The ECG, over a single cardiac cycle, has a characteristic morphology as shown in Fig 2.4 comprising a P wave, a QRS complex and a T wave. The normal ECG configurations are composed of waves, complexes, segments, and intervals recorded as voltage (on a vertical axis) against time (on a horizontal axis). A single waveform begins and ends at the baseline. When the waveform continues past the baseline, it changes into another waveform. Two or more waveforms together are called a complex. A flat, straight, or isoelectric line is called a segment. A waveform, or complex, connected to a segment is called an interval. All ECG tracings above the baseline are described as positive deflections. Waveforms bellow the baseline are negative deflections.

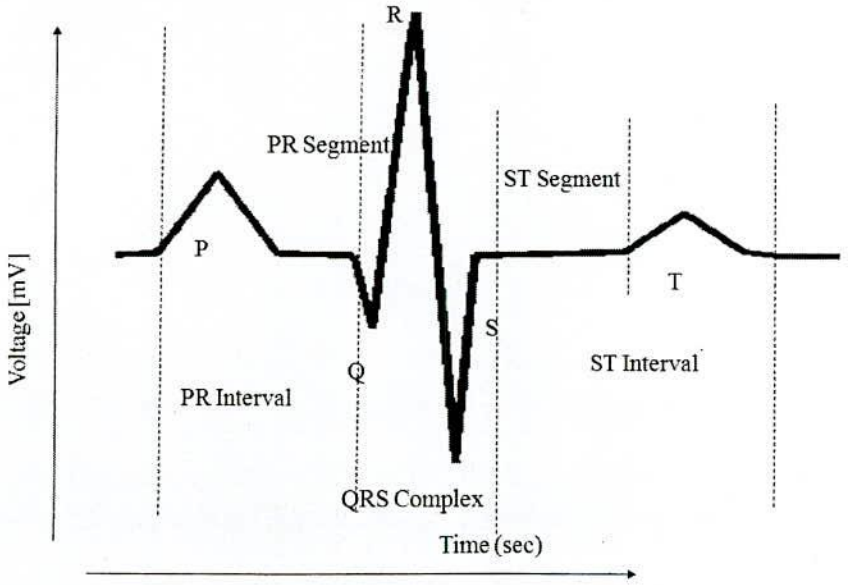

Figure 2.4: The human ECG signal over one cardiac cycle.

P wave

The propagation of the SA action potential through the atria results in contraction of the atria (depolarization), producing the P wave. (Fig 2.4).

PR interval

The PR interval begins with the onset of the P wave (Pi) and ends at the onset of the Q wave (Qi). It represents the duration of the conduction through the atria to the ventricles. It is shown in Fig 2.4. The PR Segment begins with the endpoint of the P wave (Pi) and ends at the onset of the Q wave (Qi). It represents the duration of the conduction from the atrioventricular node, down the bundle of its end through the bundle branches to the muscle. It is shown in Fig 2.3.

QRS complex

The QRS complex corresponds to the period of ventricular contraction or depolarization. The atrial repolarization signal is swamped by the much larger ventricular signal. It is the result of ventricular depolarization through the Bundle Branches and Parkinje fibres. The QRS complex is much larger signal than the P wave due to the volume of ventricular tissue involved, although some signal cancellation occurs as the waves of depolarisation in the left and right sides of the heart move in opposite directions. If either side of the heart is not functioning properly, the size of the QRS complex may increase. As shown in Fig 2.4. QRS can be measured from the beginning of the first wave in the QRS to where the last wave in the QRS returns to the baseline.

ST segment

The ST segment represents the time between the ventricular depolarisation and the repolarisation. The ST segment begins at the end of the QRS complex (called J point) and ends at the beginning of the T wave. Normally, the ST segment measures 0.12 second or less. The precise end of depolarisation (S) is difficult to determine as some of the ventricular cells are beginning to repolarise. It is shown in Fig 2.4.

T wave

The T wave results from the repolarisation of the ventricles and it has longer duration than the QRS complex because the ventricular repolarisation happens more slowly than depolarisation. Normally, the T wave has a positive deflection of about 0.5mv, although it may have a negative deflection. It may, however, be of such low amplitude that it is difficult to read. The duration of the T wave normally measures 0.20 second or less.

QT interval

The QT interval begins at the onset of the Q wave (Qi) and ends at the endpoint of the T wave (T), representing the duration of the ventricular depolarisation/repolarisation cycle. The normal QT interval measures about 0.38 second and varies in males and females and with age. As a general rule, the QT interval should be about 40 percent of the measured R-R interval. The QT interval is shown (Fig 2.4).

Table 2.1 below provides approximate values for the duration of various waves and intervals in the normal adult ECG and typical Lead II ECG features and their normal values in sinus rhythm are represented in Table 2.2.

Table 2.1: Descriptions of ECG signal components

Segment	Amplitude(mV)	Duration (Sec.)	Representation
P	0.25	0.08	Polarization of Artia
Q	25% of R		Spetal Depolarization
R	1.60		Ventricular Depolarization
P-R Interval		0.12- 0.20	Time taken SA node to travel to Ventricle
QRS Complex		0.09	Ventricular depolarization and Contraction
T	0.1 -0.5	0.16	Beginning of ventricular relaxation
S-T segment		0.05-0.15	Interval between S and T Wave

Table 2.2: Typical lead II ECG features and their normal values in sinus rhythm at a heart rate of 60 bpm for a healthy male adult [1] .

feature	Normal value	Normal limit
P width	110 ms	±20 ms
PQ/PR interval	160 ms	±40 ms
QRS width	100 ms	±20 ms
QTc interval	400 ms	±40 ms
P amplitude	0.15 mV	±0.05 mV
QRS height	1.5mV	±0.5mV
ST level	0 mV	±0.1mV
T amplitude	0.3mV	±0.2mV

Note: There are some variations among lead configurations. Heart rate, respiration patterns, drugs, gender, diseases, and ANS activity also change the values. QTc = αQT where $\alpha = (RR)^{-1/2}$. About 95% of (normal healthy adult) people have a QTc between 360 ms and 440 ms. Female durations tend to be approximately 1% to 5% shorter except for the QT/QTc, which tends to be approximately 3% to 6% longer than for males. Intervals tend to elongate with age, at a rate of approximately 10% per decade for healthy adults [1].

CHAPTER III

NOISES IN ECG

3.1 Sources of ECG Noises

Electrocardiographic (ECG) signals may be corrupted by various kinds of noise. Typical examples are [5]:

a) Power line interference
b) Electrode contact noise
c) Motion artifacts
d) Muscle contraction (electromyography, EMG)
e) Baseline drift and ECG amplitude modulation with respiration
f) Instrumentation noise generated by electronic devices used in signal processing,
g) Electrosurgical noise

and other, less significant noise sources [6] . A brief description of each noise signal listed will be given below.

a) **Power Line Interference**:

50 ±0.2 Hz mains noise (or 60 Hz in many data sets) with an amplitude of up to 50% of full scale deflection (FSD), the peak-to-peak ECG amplitude.

Typical parameters:

Frequency content	:50 or 60 Hz (fundamental in U.S 60 Hz other like Asia 50Hz) with harmonics
Amplitude	:Up to 50 percent of peak-to-peak ECG amplitude.

b) Electrode Contact Noise

Electrode contact noise is transient interference caused by loss of contact between the electrode and skin, which effectively disconnects the measurement system from the subject. The loss of contact can be permanent, or can be intermittent, as would be the case when a loose electrode is brought in and out of contact with the skin as a result of movements and vibration. This switching action at the measurement system input can result in large artifacts since the ECG signal is usually capacitively coupled to the system. With the amplifier input disconnected,

60 Hz interference may be significant. Electrode contact noise can be modeled as a randomly occurring rapid baseline transition (step) which decays exponentially to the baseline value and has a superimposed 60 Hz component. This transition may occur only once or may rapidly occur several times in succession. Characteristics of this noise signal include the amplitude of the initial transition, the amplitude of the 60 Hz component, and the time constant of the decay.

Typical parameters:

Duration	: 1 sec.
Amplitude	: maximum recorder output.
Frequency-60 Hz Time constant	: about 1sec.

c) Motion Artifacts

Motion artifacts are transient (but not step) baseline changes caused by changes in the electrode-skin impedance with electrode motion. As this impedance changes, the ECG amplifier sees a different source impedance, which forms a voltage divider with the amplifier input impedance. Therefore, the amplifier input voltage depends on the source impedance, which changes as the electrode position changes. The usual cause of motion artifacts will be assumed to be vibrations or movement of the subject. The

shape of the baseline disturbance caused by motion artifacts can be assumed to be a biphasic signal resembling one cycle of a sine wave. The peak amplitude and duration of the artifact are variables.

Typical parameters:

Duration	:100-500 ms
Amplitude	:500 percent of peak-to-peak ECG amplitude.

d) Muscle Contractions (EMG)

Muscle contractions cause artifactual millivolt-level potentials to be generated. The baseline electromyogram is usually in the microvolt range and therefore is usually insignificant. It can be assumed to be transient bursts of zero-mean band-limited Gaussian noise. The variance of the distribution may be estimated from the variance and duration of the bursts.

Typical parameters:

Standard Deviation	:10 percent of peak-to-peak ECG amplitude
Duration:	:50 ms
Frequency Content	:dc to 10 000 Hz

e) Baseline Drift and ECG Amplitude Modulation with Respiration

The drift of the baseline with respiration can be represented as a sinusoidal component at the frequency of respiration added to the ECG signal. The amplitude and frequency of the sinusoidal component should be variables. The amplitude of the ECG signal also varies by about 15 percent with respiration. The variation could be reproduced by amplitude modulation of the ECG by the sinusoidal component which is added to the baseline. .

Typical parameters:

Amplitude variation	:15 percent of peak-to-peak (p-p) ECG amplitude
Baseline variation	:15 percent of p-p ECG amplitude variation at 0.15 to 0.3 Hz.

f) Noise Generated by Electronic Devices Used in Signal Processing

Artifacts generated by electronic devices in the instrumentation system . The input amplifier has saturated and no information about the ECG can reach the detector. This can be represented by white noise and colored noise. In this case an alarm must sound to alert the ECG technician to take corrective action.

g) Electrosurgical Noise

Electrosurgical noise completely destroys the ECG and can be represented by a large amplitude sinusoid with frequencies approximately between 100 kHz and 1 MHz. Since the sampling rate of an ECG signal is 250 to 1000 Hz, an aliased version of this signal would be added to the ECG signal. The amplitude, duration and possibly the aliased frequency should be variable.

Typical parameters:

Amplitude	:200 percent of peak-to-peak ECG amplitude.
Frequency Content	: Aliased 100 kHz to 1 MHz Duration-1-10s

3.2 Different noise under study

In this research the following noises are studied. Electromyographic interference because of its random properties and high frequency content. Baseline drift due to respiration because of its low frequency properties. In addition, white noise, colored noise, real muscle artifact, electrode movement and composite of the above mentioned noise are studied in this chapter.

3.2.1 Synthetic noises

White noise is a random signal with a flat power spectral density. It has all frequency components. Flicker noise or color noise is a type of low-frequency electronic noise with an inversely proportional power spectral density compared with the frequency. Resistance fluctuation is the main reason for flicker noise generation and that's why all resistors has flicker noise. For the current study, we have modeled the noise color by a single parameter representing the slope of a spectral density function that decreases monotonically with frequency by $S(f) \propto \frac{\sigma^2}{f^{\beta}}$.

Where f is the frequency, σ^2 is the variance of the original signal and β is the slope; a measure of noise color. White noise (β=0), pink or flicker noise (β=1), and brown noise or the random walk process (β=2), are three of the most commonly referenced noises .White noise and color noise are simulated having 3dB input SNR using MATLAB.

3.2.2 Real Noise

Real noises are extracted from the noise stress test database in MIT-BIH [7]. Low-amplitude muscle noise is common in ECG. Different noises was tested on the ECG data recorded from BIOPAC data acquisition system [8]. The noisy signal was generated by adding Baseline Wander(BW), Electrode Movement(EM), and Motion Artifact (MA) (Noise Stress Test Database of MIT-BIH) and white and color noise were added to the clean ECG signals . Different types of noisy ECG signal are shown in Fig. 3.1.

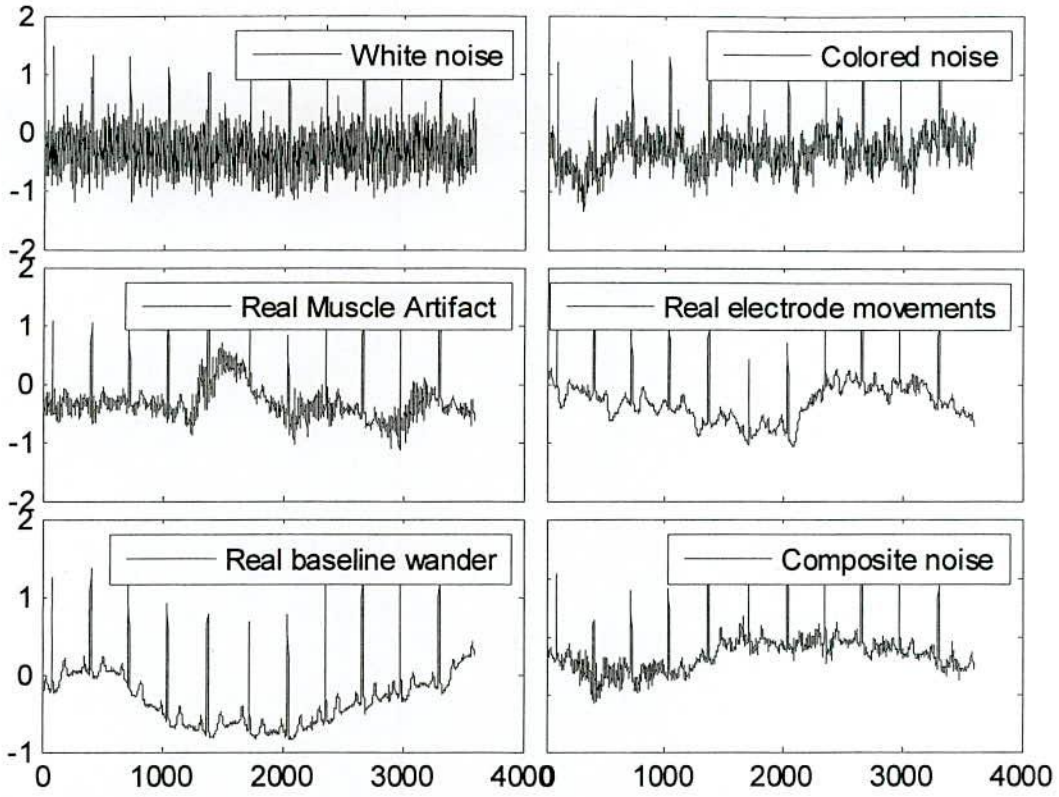

Figure 3.1: Different types of noisy ECG signal. Original record are collected from MIT-BIH arrythmia database of record no 101.

3.3 Necessities of ECG Denoising

Cardiovascular diseases (CVDs) are the most widespread cause of death in many countries all over the world. Electrocardiogram (ECG) is one of the most basic useful, easily available and low cost tools for the early diagnosis and evolution of many cardiac problems. ECG signal can potentially be corrupted by various types of noises which may lead to incorrect diagnosis. According to World Health Organization (WHO) 2003 reports CVDs made up 16.7 million, or 29.2% of total global deaths. It is widely accepted that, ECG is one of the reliable and low cost tools for detecting most of the CVDs. Like other electrical signal, ECG signals are corrupted by various kinds of noise. The presence of noise in signal systems can severely affect interpretation of the data and lead to an incorrect diagnosis. So ECG denoising is necessary to prevent misdiagnosis.

CHAPTER IV

ECG SIGNAL MODELING: A SIMPLE MATHEMATICAL APPROACH

4.1 ECG MODEL

Electrocardiogram (ECG) is a measurement of bio-electric potential produced by rhythmical cardiac activities contraction and relaxation of the cardiac muscle produced at SA node. This electric potential associated with the cardiac cycle can be detected at the surface of the body, amplified and recorded as a time record of each cardiac cycle. Different cardiac function such as heart rate, abnormality of rhythm can easily be identified by ECG that's why ECG signal modeling and processing is the most significant topic in biomedical signal analysis.

Different techniques have been developed in the past for modeling of ECG. For feature extraction and data compression a pole-zero models of the ECG was represented by [9] . Another research [10] reported ECG signals with pole-zero models, the poles and zeros form clusters and the clusters can be related to the constituent waves of the ECG. Transform-type methods like nonlinear transform using multiplication backward difference for detecting QRS. Another Orthonormal basis of Hermite functions for pattern recognition purposes in ECG was stated by [11] using only QRS complex. Polynomial approximation modeling was used to model the ECG for data compression [12]. Other researchers like [13] used parametric modeling of the discrete cosine transform of the ECG for data compression. However, this types of modeling do not provide a direct representation of the constituent waves in the ECG as medical experts are needed for making diagnoses.

Chip Away Decomposition (ChAD) algorithm which is an iterative method for Gaussian parameter determination was used for decomposing and representing the ECG model by [14]. References [15] [16]improved the proposed model in Reference [17] with accounting for T wave asymmetry. Modeling of ECG with seven Gaussian functions have been investigated by Clifford et al. [18] by means of 3D state-space model which require numerical integration using a fourth-order Runge-Kutta method. S. Paravena et al. [19] used a large number of Gaussian with no base line drift factor. They used 4 to 133

Gaussian function based on minimum bank method and zero crossing method. But fitting this model to the real ECG signal, starting and end point of any interval using zero crossing method is not efficient. Moreover, increasing number of Gaussian functions require much time to run the program. Authors in [20] proposed a model using Gaussian function but they cannot represent QRS wave individually as well as it is unable to fit with the real ECG at a significant level. They used double differentiation of the Gaussian function which is time consuming and need complex mathematical operation. The fitting techniques were inefficient because they were not capable to fit any negative values in their model which was quite common in real data.

This work proposes a Gaussian wave base model which can simulate ECG wave as well as P, Q, R, S and T wave individually and is very simple as compared to compared to earlier mentioned model. In addition, there is no needing for preprocessing the baseline like [20], the model can automatically shift the baseline as normally exist in the real ECG. The coefficient of the model is calculated section by section by nonlinear least square technique using gauss-Newton algorithm. The performance of the proposed model and fitting algorithm are evaluated by using several morphologically different waveforms from recorded and collected ECG database thereby exemplifying model performance for each morphology. To understand the effectiveness of fitting, goodness of fitting are calculated. Real data are pre-processed for better fitting by using wavelet base filtering with soft thresholding technique. Finally, the frequency-domain analysis of ECG signals is demonstrated.

4.1.1 Proposed Approach

ECG signal is the combination of P, Q, R, S and T waves and it has more and less symmetric "bell curve" shape that quickly falls toward both sites which is one of the characteristic of Gaussian wave. Gaussian function is widely used in signal processing where the signals are illustrated as normal distribution. The modeling approaches, would prefer a model in a way that the individual waves and the anomalies between them are represented by a small set of model parameters, and model coefficients should correspond to a particular wave of interest.

If $i \in (P,Q,R,S,T)$ than Gaussian wave for each component of ECG wave have following parameter: A_i is height of curves peak, t_i is the center position of the peak and B_i controls the width then ECG components can be written as :

$$\text{P wave}: A_p e^{-\left(\frac{(t-t_p)^2}{2B_p^2}\right)} + c_p \tag{4.1}$$

$$Q \text{ wave} : A_{q_1} e^{-\left(\frac{(t-t_{q1})^2}{B_{q1}^2}\right)} + A_{q_2} e^{-\left(\frac{(t-t_{q2})^2}{B_{q2}^2}\right)} + c_q \tag{4.2}$$

$$R \text{ wave} : A_r e^{-\left(\frac{(t-t_r)^2}{2B_r^2}\right)} + c_r \tag{4.3}$$

$$S \text{ wave} : A_s e^{-\left(\frac{(t-t_s)^2}{2B_s^2}\right)} + c_s \tag{4.4}$$

$$T \text{ wave} : A_t e^{-\left(\frac{(t-t_t)^2}{2B_t^2}\right)} + c_t \tag{4.5}$$

Simply the general equations of 4.1 to 4.5 can be written as

$$f_i = \sum_{i \in p,r,s,t} A_i e^{-\left(\frac{(t-t_i)^2}{2B_i^2}\right)} + \sum_{i \in q, j=1}^{j=2} A_{ij} e^{-\left(\frac{(t-t_{ij})^2}{B_{ij}^2}\right)} + c_i \tag{4.6}$$

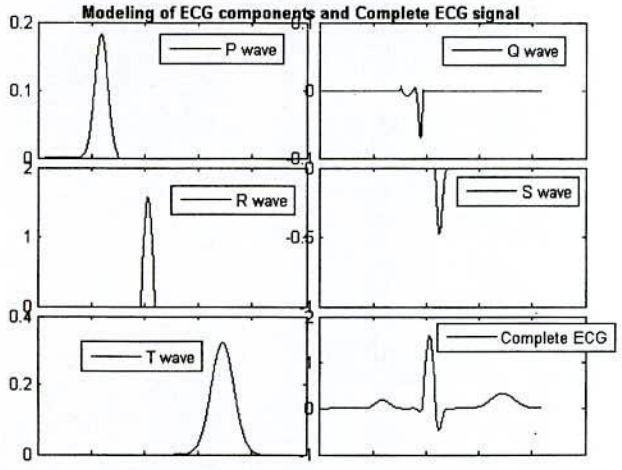

Figure 4.1: ECG component and complete ECG signal. Here individual ECG components are placed to their respective places using shifting and zero padding techniques.

If we perform normal sum of Eq. (4.6), the individual P, Q, R, S, T component of ECG will be overlapped with each other wave. To solve this problem, ECG components are fitted to their right position using shifting and zero padding method (shown in Fig. 4.1). Here, c_i can be used for model fitting to adjust the baseline, noisy signal generation which is an extra feature of this model.

4.1.2 Novelty of The Proposed Approach

Though generating ECG by using signal like Gaussian is done by [19] [20] the novelty of our proposed model are as follows:

a. The proposed system can generate ECG and is capable of simulating various kind of practical phenomena such as brachycardia (slow heart rate), tachycardia (fast heart rate) and HRV (Heart Rate Variability) etc.

b. It does not need three dimensional state space which is difficult for realization and simulation.

c. An extra baseline parameter c_i of the model reduces the pre-processing of signal by automatically adjust the baseline.

d. Noisy ECG signal can be modeled simply by adding a noise parameter in c_i with the model.

This section discusses the experimental recoding of ECG signal, preprocessing, fitting procedures, FFT method, and performance evaluation parameters.

4.2 Material and Methods

4.2.1 Experimental Recording of ECG

The experiment is performed to collect the data for this research work. The subject is a male of 26 years old with no known cardiovascular disorder. For ECG and measurement, required equipments are BIOPAC electrode lead set (SS2L), BIOPAC disposable vinyl electrodes (EL503), BIOPAC data acquisition unit (MP36) [8] [76] with cable and power. For ECG measurement, white lead was placed on right forearm, red lead on the left leg and the black lead was placed on right leg as shown in Fig. 4.2. Subjects was seated in a chair relaxing and asked to be as still as possible to ensure lower motion artifact and EMG signal on the data. After running calibration sequence ECG data was recorded.

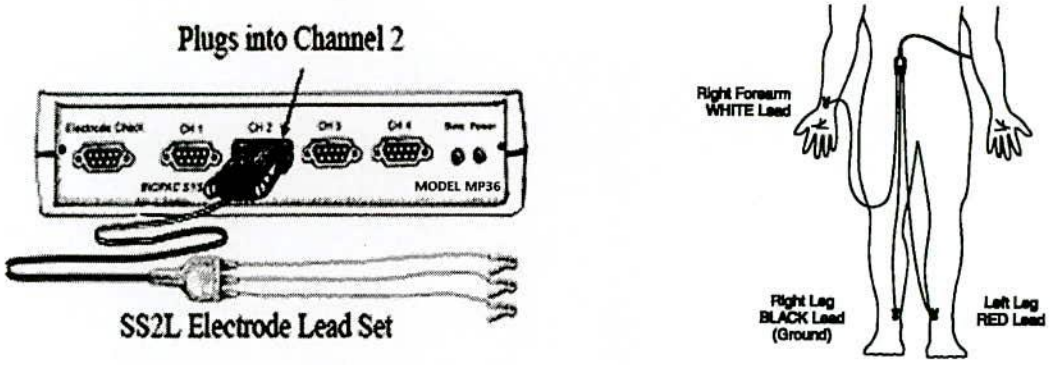

(a) (b)

Figure 4.2: (a)MP36 BIOPAC system (b)Placement of lead in ECG measurement.

4.2.2 Preprocessing

The acquired ECG data are preprocessed to remove noise, artifacts, and baseline wander using Savitzky-Golay Filtering [21][73].To this end, two frequency-selective fourth-order Butterwort filters [22] are used: one high-pass filter with cutoff frequency at 0.5Hz and one low-pass filter with cutoff frequency at 90 Hz. To suppress the interferences from the power line grid, a notch filter centered around 50 was used. Again, this filter is implemented as a fourth-order Butterworth filter like [23].

4.3 Nonlinear Fitting

For fitting the mathematical model with the real world data statistical hypothesis testing like: test of normality of residuals, chi square test, analysis of variance, least square test etc [24] is needed. As it observed that, ECG model is nonlinear in the coefficients. So the nonlinear least square techniques can be the best choice for this fitting. Nonlinear models are more difficult to fit than linear models because the coefficient cannot be estimated using simple techniques instead an iterative approaches required to solve this problem.

Consider that an ECG function $y=f(x)$ of a variable of x tabulated at i values, where $y_1=f(x_1)$, $y_2=f(x_2)$ ..... $y_i=(x_i)$. Moreover, assuming that the known analysis form the function depending on j parameters $f(x;\phi_1,\phi_2,.....,\phi_j)$ and the set of i equation will be

$$\left.\begin{aligned} y_1 &= f(x_1;\phi_1,\phi_2,\ldots\ldots\ldots,\phi_j) \\ y_2 &= f(x_2;\phi_1,\phi_2,\ldots\ldots\ldots,\phi_j) \\ &\vdots \\ y_i &= f(x_i;\phi_1,\phi_2,\ldots\ldots\ldots,\phi_j) \end{aligned}\right\} \tag{4.7}$$

We have to solve the equation to obtain the value of $\phi_1,\phi_2,\ldots\ldots\ldots\ldots,\phi_j$ which satisfies our model properly. At first an initial value is picked for ϕ_k and defined

$$d\beta_k = y_k - f(x_k;\phi_1,\phi_2,\ldots\ldots\ldots,\phi_j) \tag{4.8}$$

And then the estimation for the change $d\phi_k$ needed to reduce $d\beta_k$ to 0

$$d\beta_k = \sum_{l=1}^{j} \frac{df}{d\phi_l} d\phi_l \Big|_{x_k\phi} \tag{4.9}$$

For $k=1,2,\ldots,i$ where

$$\phi \equiv (\phi_1,\phi_2,\ldots,\phi_j) \tag{4.10}$$

This element can be written as a $i \times j$ matrix of partial derivatives of

$$A_{kl} = \begin{vmatrix} \left.\frac{df}{d\phi_1}\right|_{x_1\phi} & \ldots & \ldots & \ldots & \left.\frac{df}{d\phi_j}\right|_{x_1\phi} \\ \left.\frac{df}{d\phi_1}\right|_{x_2\phi} & \ldots & \ldots & \ldots & \left.\frac{df}{d\phi_j}\right|_{x_2\phi} \\ \vdots & \ddots & & & \\ \vdots & & \ddots & & \\ \left.\frac{df}{d\phi_1}\right|_{x_i\phi} & \ldots & \ldots & \ldots & \left.\frac{df}{d\phi_j}\right|_{x_i\phi} \end{vmatrix} \tag{4.11}$$

Then,

$$d\beta_k = A_{kl} d\phi_l \tag{4.12}$$

And the brief equation is

$$d\beta = Ad\phi \tag{4.13}$$

If by defining $a=A^TA$ and $b=A^Td\beta$

We find,

$$a\,d\phi = b \tag{4.14}$$

Then Eq. (4.14) is solved for $d\phi$ using Gaussian elimination techniques. This offset is applied to ϕ and a new $d\phi$ is calculated. By interactively applying this procedure until the elements of $d\phi$ become smaller than desired limit, a solution is obtained. The sum of square residuals is calculated by $R^2 = d\beta.d\beta$ after the final iteration.

4.4 Performance Evaluation Parameters

4.4.1 Fourier Transform

As Fourier transform of a Gaussian function is also a Gaussian function [25] and the Fourier transform of (4.6) can be expressed as [77]:

$$A_i e^{-b_i(t-t_i)^2} \overset{FT}{\Leftrightarrow} \underbrace{A_i\sqrt{\frac{\pi}{b_i}}\,e^{-\omega^2/4b_i}}_{Magnitude}\;\underbrace{e^{-j\omega t_i}}_{Phase} \tag{4.15}$$

$$\text{Where, } b_i = \begin{cases} \dfrac{1}{2B_i^2} & i \in p,r,s,t \\ \dfrac{1}{B_i^2} & i \in q \end{cases} \tag{4.16}$$

As can be observed from Eq. (4.15), there is an inverse relationship width b_i between time domain and frequency domain, because frequency domain Gaussian function $\hat{X}(\omega)$ is not shifted. So $\hat{X}(\omega)$ is simply the sum of the corresponding ECG component.

4.4.2 Coherence

The magnitude squared coherence (MSC) estimate is a function of frequency with values between 0 and 1 that indicates how well the model ECG corresponds to real ECG at each frequency. The MSC estimate C_{xy} of the input signals (x and y) using Welch's averaged, modified periodogram method [26][74]. The MSC is nothing but a function of the power spectral densities (P_{xx}(f) and P_{yy}(f)) of x and y and the cross power spectral density (P_{xy}(f)) of x and y.

$$C_{xy} = \frac{|P_{xy}(f)|^2}{P_{xx}(f)P_{yy}(f)} \tag{4.17}$$

In this research; x, y represents the model and real ECG signal respectively and x and y must be the same length.

4.4.3 Power spectral density (PSD)

Power Spectral Density (PSD), which describes how the power of a signal or time series is distributed with frequency [26] [74]. It shows at which frequencies variations the signal power are strong and at which frequencies variations the signal power are weak. Energy can be obtained within a specific frequency range by integrating PSD within that frequency range. Computation of PSD is done directly by the method called FFT or computing autocorrelation function and then transforming it.

4.4.4 Cross-correlation coefficient

If x(n) be the recorded or collected ECG signal and $x_m(n)$ be the ECG signal generated by the mathematical model, then cross-correlation coefficient ρ between $x(n)$ and $x_m(n)$ is given by [1]:

$$\rho = \frac{\langle [x(n) - \mu_x][x_m(n) - \mu_m] \rangle}{\sigma_x \sigma_m} \tag{4.18}$$

Where $\langle \bullet \rangle$ denotes the average calculated by summing over the observed time series, indexed by n. where μ_x and σ_x are the mean and standard deviation of *x(n)*, and μ_m and σ_m are the mean and standard deviation of $x_m(n)$. A value of $\rho \sim 1$ reflects a strong correlation, $\rho \sim -1$ implies a strong anticorrelation, and $\rho \sim 0$ indicates that *x(n)* and $x_m(n)$ are uncorrelated. This means that a value of $\rho = 1$ suggests that model and real ECG are identical.

4.4.5 Error Evaluation Parameters

If *x(n)* be the recorded or collected ECG signal and $x_m(n)$ be the ECG signal generated by the mathematical model, then Mean Square Error (MSE) is defined as [27]:

$$MSE = \frac{1}{N}\sum_{n=0}^{N-1}[x(n) - x_m(n)]^2 \tag{4.19}$$

The normalized form of MSE is $$NMSE = \frac{\sum_{n=0}^{N-1}[x(n) - x_m(n)]^2}{\sum_{n=0}^{N-1}[x(n)]^2} \tag{4.20}$$

Another measurement is Root Mean Square Error, which is

$$RMSE = \sqrt{\frac{1}{N}\sum_{n=0}^{N-1}[x(n) - x_m(n)]^2} \tag{4.21}$$

The Normalized version of RMSE is $$NRMSE = \sqrt{\frac{\sum_{n=0}^{N-1}[x(n) - x_m(n)]^2}{\sum_{n=0}^{N-1}[x(n)]^2}} \tag{4.22}$$

Percent Root Mean Difference (PRD) can be determined by Eq. (4.23).

$$PRD = \sqrt{\frac{\sum_{n=0}^{N-1}[x(n) - x_m(n)]^2}{\sum_{n=0}^{N-1}[x(n)]^2}} \times 100\% \tag{4.23}$$

4.5 Evaluation of the model

To evaluate the performance of our model we compared our ECG model with a healthy subject's ECG recorded by BIOPAC data acquisition system. The model parameters (Table 4.1) were calculated by nonlinear least square technique using Gauss-Newton algorithm having 95% confidence level to fit the model with Real ECG signal these parameter were used. The comparison of generated and real ECG was shown in Fig. 4.3.

Table 4.1: Coefficient to fit the model with BIOPAC recorded ECG

		A_i	B_i	t_i	c_i
P		0.182	24.5	237	-0.05607
Q	**J=1**	-1.6	278.6	27.02	1.496
	J=2	-0.1157	12.58	78.44	
R		107.4	29.11	55.79	-1.278
S		-0.4705	9.622	14.43	-0.0682
T		0.3232	41.98	179.5	-0.0479

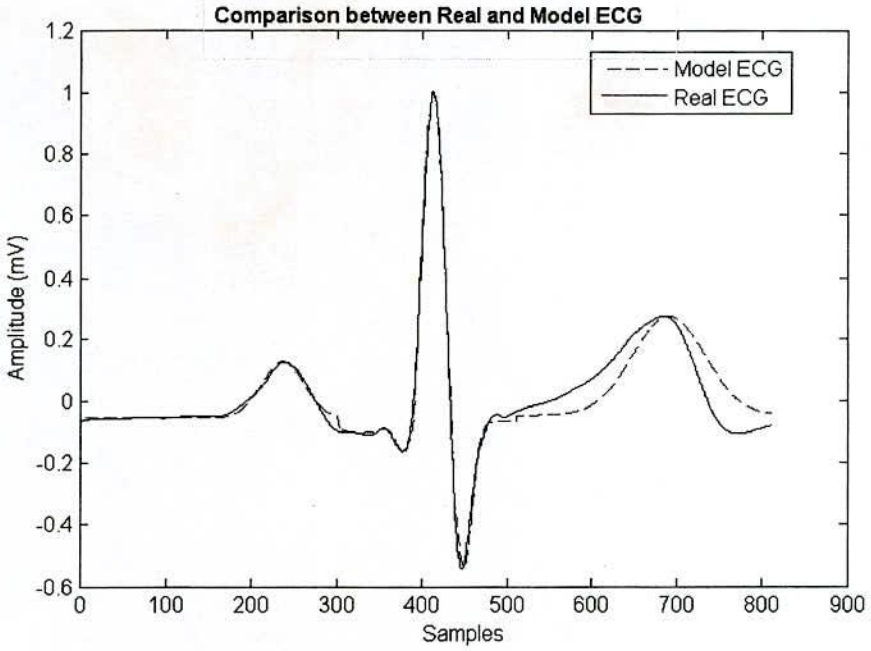

Figure 4.3 : Comparison between real and model ECG.

The frequency-domain evaluation of the model also represented in Fig.4.4, which showed the almost same analytical frequency spectrum generated by Discrete Fourier Transform (DFT) between real and model ECG.

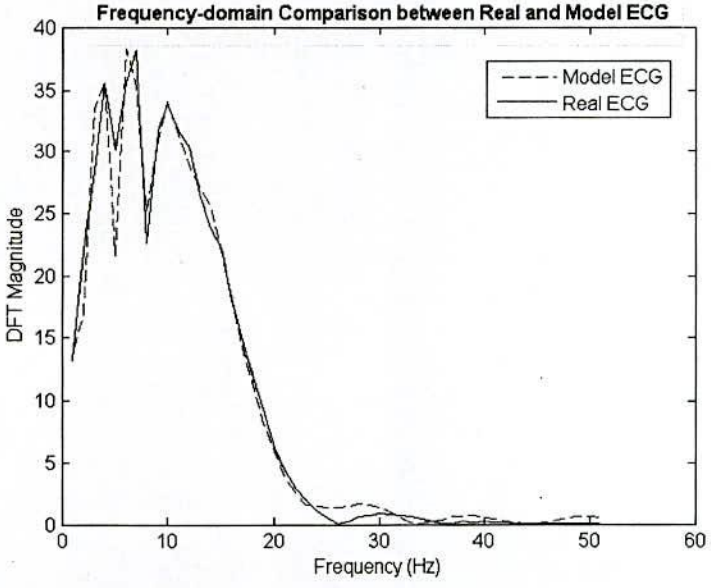

Figure 4.4: Frequency –domain comparison between real and simulated model.

This model not only simulates normal ECG but can generate beat abnormalities of heart like brachycardia and tachycardia. From Fig. 4.5, brachycardia is simulated for 5 sec possessing 4 beat. So the beat per minute (BPM) is 48. Sinus rhythm and tachycardia were simulated in the same way.

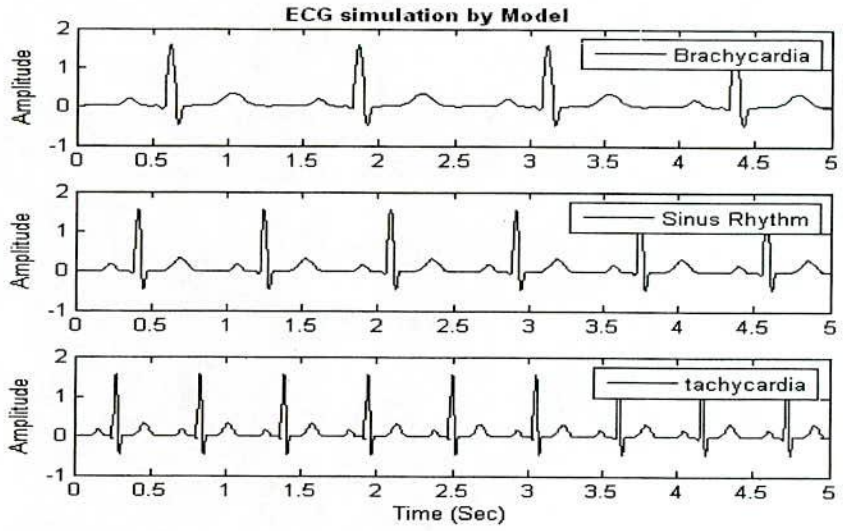

Figure 4.5: ECG simulation by model for 5 Sec. For brachycardia with BPM 48, sinus rhythm with BPM 72, tachycardia with BPM 108.

In addition, morphologically different physiological or pathophysiological conditions can also be simulated by the model. For example, ECG waveform was selected from the MIT-BIH Intracardiac atrial fibrillation database *(iafdb)* for atrial fibrillation modeling [7]. By properly fitting the model with the selected waveform, it was clear that the model can satisfy the atrial fibrillation condition represented by Fig. 4.6.

The proposed model was capable of replicating many important features of the human ECG wave. Moreover, many of the morphological changes such as atrial fibrillation and tachycardia, brachycardia can be fitted by selecting proper model parameter. Moreover, noisy ECG signal can be modeled by simply adding a noise parameter with the model. A realistic ECG database can be created by fitting the model with individual subject's ECG. This can be used for further analysis and for education and research purpose.

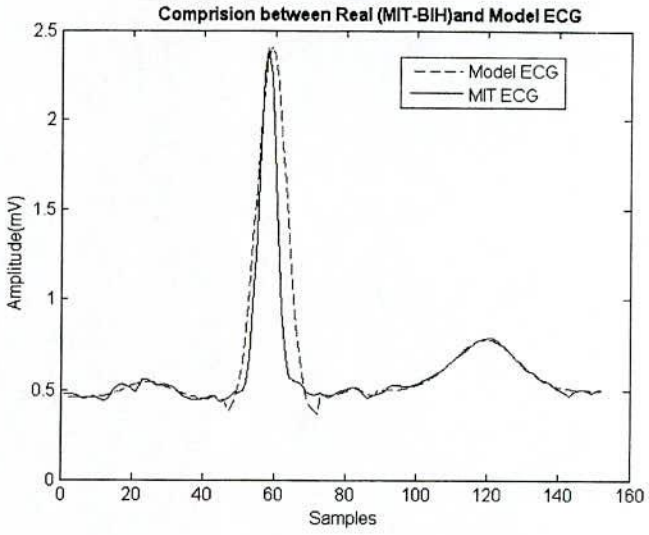

Figure 4.6 : Modeling of atrial fibrillation of MIT-BIH iafdb database, Record No: iafl_svcm(age 81, female).

Base line drift factor in the model helps the model to fit the model effectively. It may be omitted if the real ECG's base line lies on the zero line. However, the model fits the normal ECG with MSE of 0.0023 and atrial fibrillation with MSE of 0.0291. In addition, higher cross-correlation coefficient of 0.9208 between model and real ECG indicates the outstanding performance of the model .The proposed model can be improved for better fitting, model-based denoising, compression and neural network based classification etc. which is currently under investigation. Finally, it hope that this simple model will provide an efficient tool for testing and processing of the ECG signals with different level of noise and/or motion artifact.

4.6 Noisy ECG Generation

As real ECG is contaminated by different noises, so noise should be taken into account for more realistic modeling. Various noises are modeled in the following session.

Another feature of the model is that, it can generate realistic and simulated noisy ECG signal. Additional C_i in Eq. (4.6) can be used as noise parameter in the model. Different noisy ECG signals were simulated for the input SNR of 3dB in Fig 4.7.

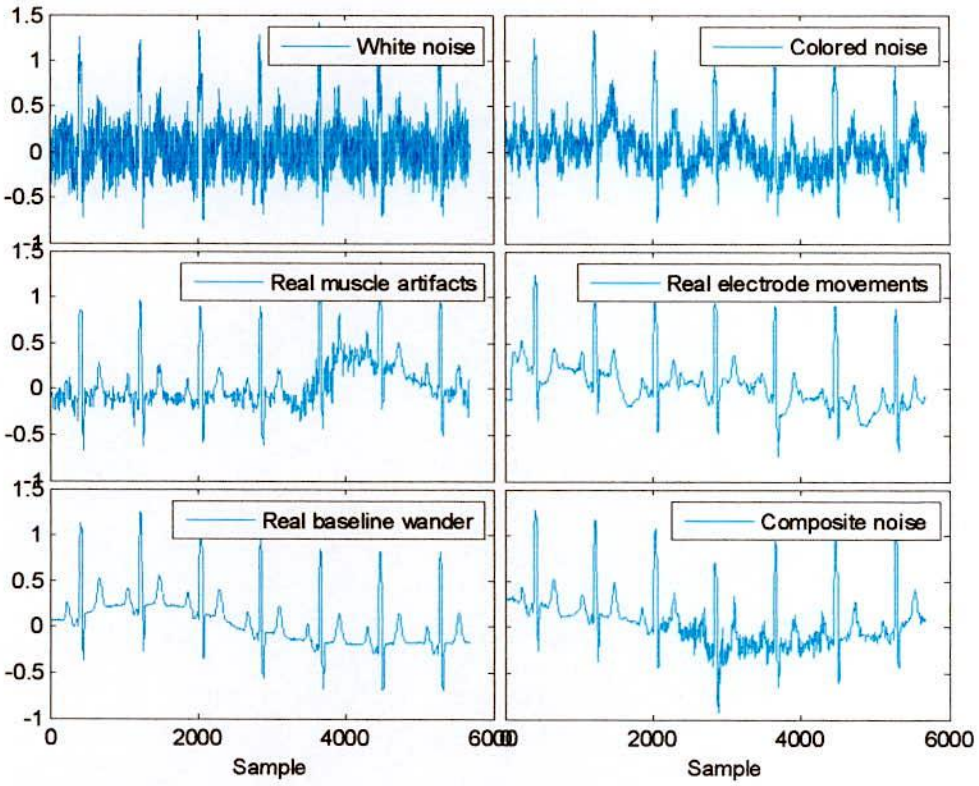

Figure 4.7: Different types of noisy ECG signal.

The model was not only evaluated in the time domain but also in the frequency domain. Figure 4.8 and Fig.4.9 showed the power spectral density (PSD) and magnitude square coherence (MSC) respectively.

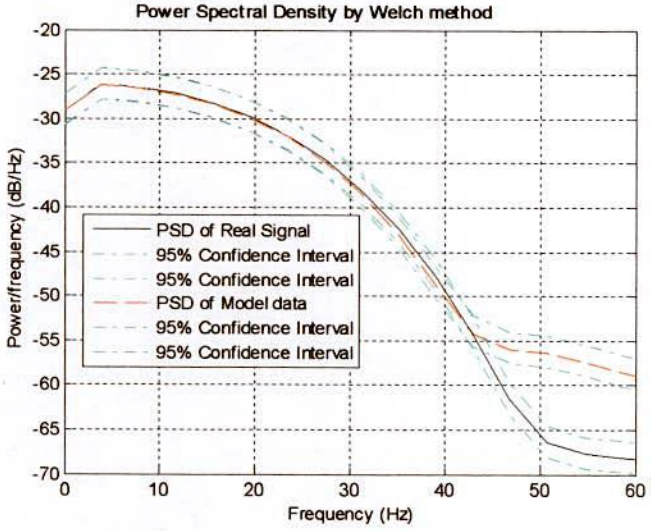

Figure 4.8: Power spectral Density of Real and model signal using Welch method.

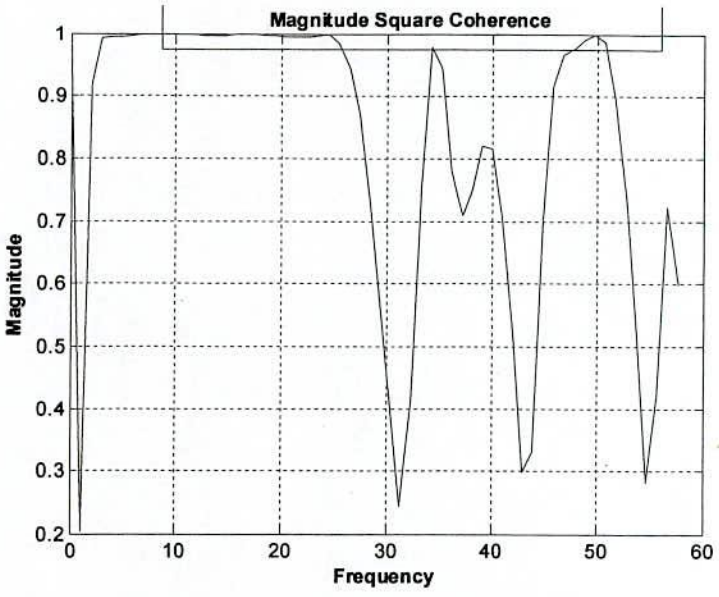

Figure 4.9: Magnitude Square Coherence between real and model Signal.

In Fig 4.8, the model and real ECG were reasonably similar and the MSC in Fig 4.9, was exists 1 in most of the frequencies which was a better indication of the proposed model. By using Eqns. (4.19)~(4.23), MSE, NMSE, RMSE, NRMSE and PRD for normal and atrial fibrillated ECGs were shown in table 4.2.

Table 4.2: Statistical analysis of the model

Goodness of fitting	Value (BIOPAC)	Value (MIT-BIH)
MSE	0.0023	0.0291
NMSE	0.0584	0.0616
RMSE	0.0485	0.1705
NRMSE	0.0034	0.0038
PRD	0.3412	0.3796

CHAPTER V

ECG DENOISING TECHNIQUES

As mentioned earlier that different noises can be contaminated with ECG signal. So denoising is necessary. In this chapter different denoising techniques are discussed.

5.1 Wiener filtering

Wiener filter theory provides for optimal filtering by taking into account the statistical characteristics of the signal and noise processes. The filter parameters are optimized with reference to a performance criterion. The output is guaranteed to be the best achievable result under the conditions imposed and the information provided. The Wiener filter is a powerful conceptual tool that changed traditional approaches to signal processing.

The noise *n(t)* is uncorrelated with the ECG signal *d(t)* . Then the corrupted ECG can be represented as: $x(t) = d(t) + n(t)$ (5.1)

where $X(\omega)$, $D(\omega)$, $N(\omega)$ represent the Discrete Fourier Transform of *x(t), s(t) , n(t)* respectively. The frequency domain version of Eq. 5.1 is as follows:

$$X(\omega) = D(\omega) + N(\omega) \tag{5.2}$$

$$|X(\omega)|^2 = |D(\omega)|^2 + |N(\omega)|^2 \tag{5.3}$$

Under the assumption of stationary noise uncorrelated with the target ECG signal, we have an alternative stochastic optimization method to suppress noise, based on minimizing the mean square error between estimated object signal value $X(\omega)$ and the original signal value $D(\omega)$. The formulation of the optimal Wiener filter is as follows.

$$W_x(\omega) = \frac{S_d(\omega)}{S_d(\omega) + S_n(\omega)} \tag{5.4}$$

Where $S_d(\omega), S_n(\omega)$ represent the estimated power spectra of the object signal and the background noise, which are assumed uncorrelated and stationary. In the pseudo stationary

case of ECG, we again resort to the frame based analysis where for each frame, the transfer function of the Wiener filter is calculated and the ECG is recovered through:

$$\hat{D}(\omega) = X(\omega)\hat{W}_x(\omega) \tag{5.5}$$

Obviously the Wiener filter requires prior knowledge of both ECG and noise statistics and they have to be estimated in real practice. By studying [1] we see that we either need a good model of the noise spectrum S_n, or a good model of the ECG itself, such as the ideal underlying source signal, $S_x = S_d + S_n$. The noise component in an ECG is highly unpredictable and often drive by exogenous impulses, such as electrode motion, that have little or no correlation with the current ECG source [1]. Therefore, in the application of the Wiener filter to ECG filtering, it is more practical to make an approximate model of the ECG and use this model to estimate the power spectrum of the signal shown in Fig 5.1.

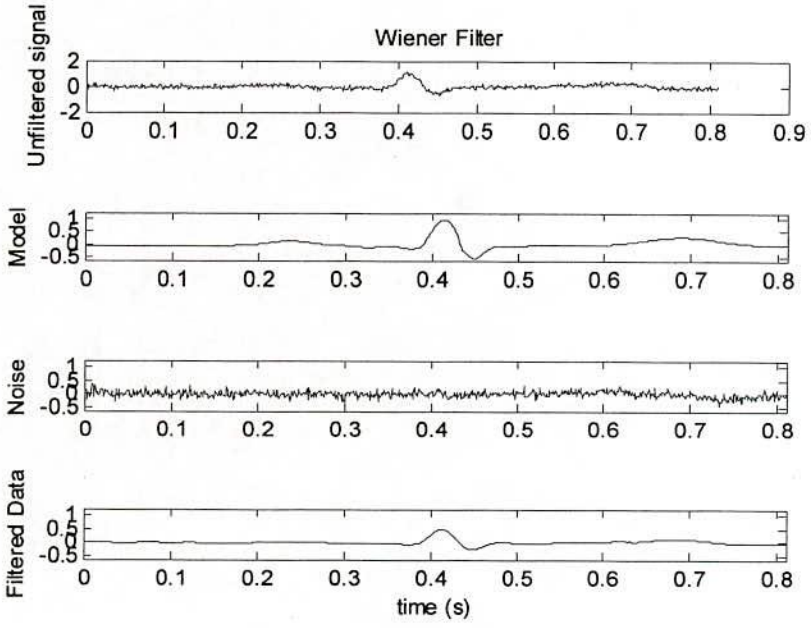

(a)

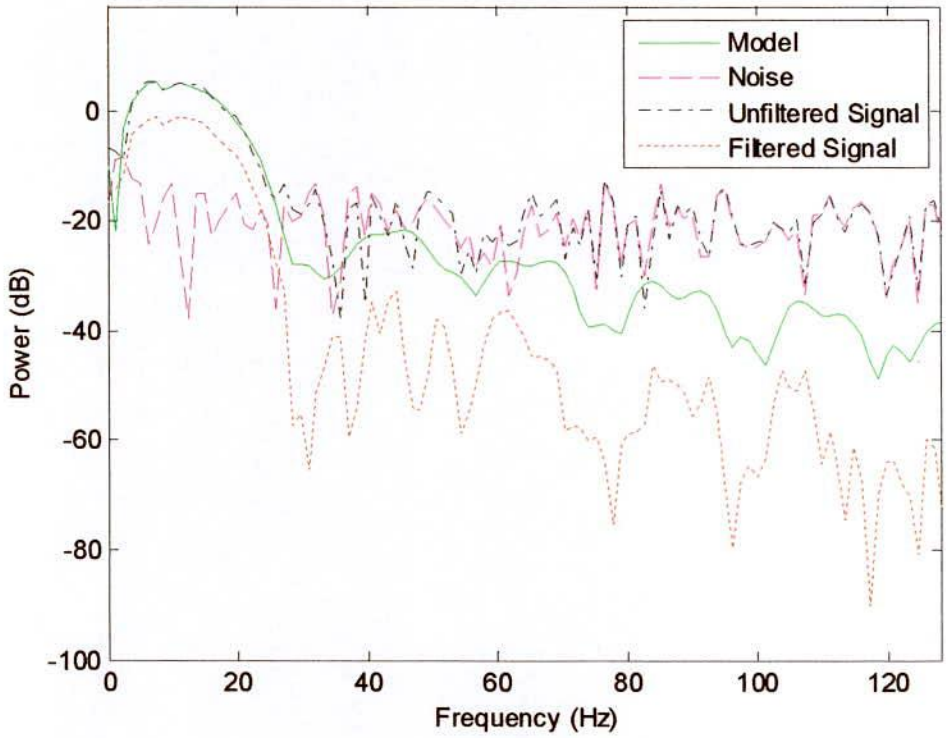

(b)

Figure 5.1: (a) Application of Wiener filter to a noisy ECG signal of SNR 5dB. (b) Power spectral density of different signal during wiener filtering process.

Unfortunately, one of the Wiener filter assumptions is that both the signal and noise are statistical (not deterministic) or stationary signals. Since the coordinated ensemble cardiac activity that manifests as an ECG appears to have some deterministic or non-stationary component, the performance of the optimal Wiener filter is diminished. In addition, a Wiener filter is not an adaptive filter because the theory behind this filter assumes that the inputs are stationary *i.e.* its joint probability distribution does not change when shifted in time or space. Consequently, parameters such as the mean and variance, if they exist, also do not change over time or position. More details can be get in [28]

5.2 Adaptive filter: LMS(Least Mean Square) filter

An adaptive filter is one whose coefficients changes with time. The LMS Filter can be implemented by an adaptive FIR filter algorithm. It is a gradient descent algorithm; it adjusts the adaptive filter taps modifying them by an amount proportional to the

instantaneous estimate of the gradient of the error surface. It estimates the filter weights, or coefficients *w(n)*, needed to minimize the error, *e(n)*, between the output signal *y(n)* and the desired signal, *d(n)* [29] [30] as shown in Fig 5.2 and the output denoised ECG is shown in Fig 5.3.

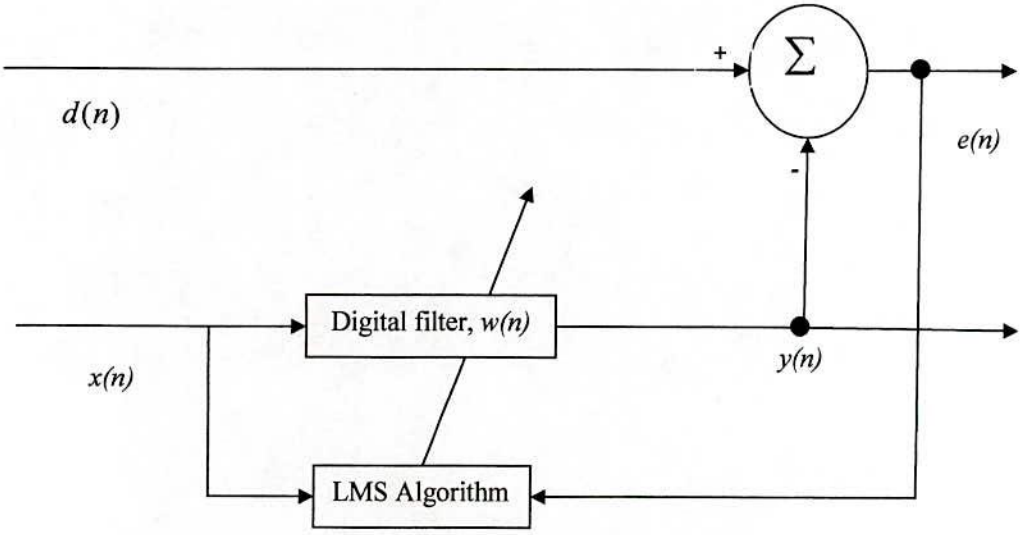

Figure 5.2: Block diagram of LMS filter.

This algorithm is defined by the following equations.

$$y(n) = w^T(n-1)x(n) \tag{5.6}$$

$$e(n) = d(n) - y(n) \tag{5.7}$$

$$w(n) = w(n-1) + f(x(n), e(n), \mu) \tag{5.8}$$

The weight update function for the LMS adaptive filter algorithm is defined as

$$f(x(n), e(n), \mu) = \mu e(n) x^*(n) \tag{5.9}$$

The variables are as follows.

Variable	Description
n	The current time index
$x(n)$	The vector of buffered input samples at step n
$x^*(n)$	The complex conjugate of the vector of buffered input samples at step n
$w(n)$	The vector of filter weight estimates at step n
$y(n)$	The filtered output at step n
$e(n)$	The estimation error at step n
$d(n)$	The desired response at step n
μ	The adaptation step size

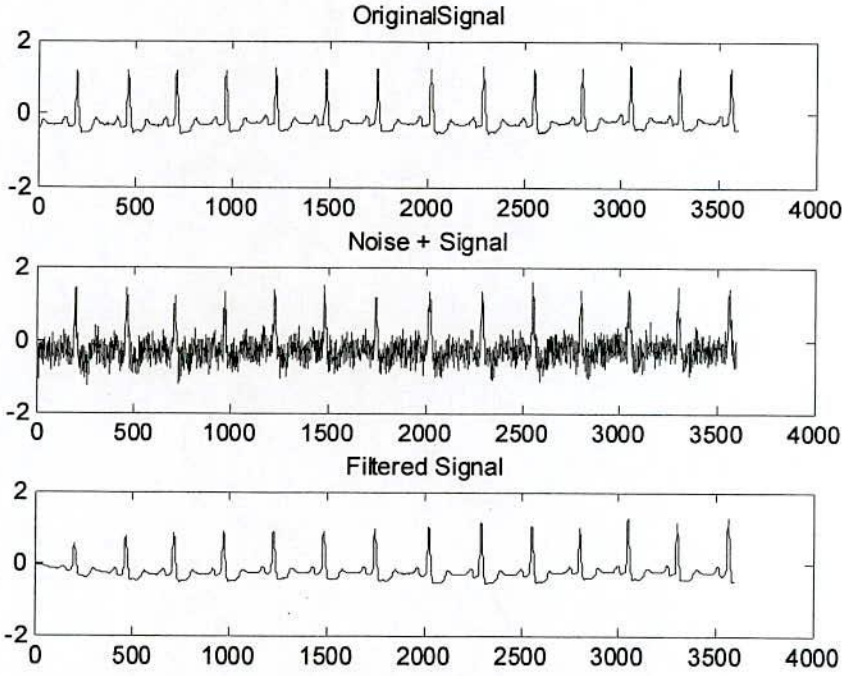

Figure 5.3: Denoising using LMS algorithm of step size 0.005 . Here record are taken from MIT-BIH arrhythmia database (Record no 105) .

The LMS filter is a simple and efficient approach for adaptive noise cancellation; however it is not appropriate for fast-varying signals like ECG due to its slow varying convergence and due to the difficulty in selecting the correct value for the step size μ [28].

5.3 Wavelet Transform

Another method for isolating transient (nonstationary) changes in a time series involves combining the time-domain and frequency-domain analysis of a signal. Such an approach has the advantage of combining both these paradigms to facilitate filtering of both persistent signal sources within the observation, and short transient sources of noise. Joint time-frequency analysis (JTFA) is then essentially a transformation of an N-point M-dimensional signal (usually where M = 1 for the ECG) into an M + 1-dimensional signal [1]. The short-time Fourier transform (STFT) is a classic example of this type of transformation which involves repeated FT calculations over small windows that are stacked up over time to construct a spectrogram(a plot of frequency against time) [1].

The wavelet transform (WT) is a popular technique for performing JTFA and belongs to a family of JTFA techniques that include the STFT, the Wigner Ville transform (WVT), the Zhao-Atlas-Marks distribution, and the Hilbert transform (All the JTFA techniques have been unified by Cohen [31]).

Unfortunately, all except WT suffer from significant cross-terms which reduce their ability to locate events in the time-frequency plane. Reduced interference distribution techniques such as the exponential or Choi-Williams distribution, the pseudo WVT, and the Margenau-Hill distribution, have been developed to suppress the cross terms to some extent, but in general, they do not provide the same degree of (time or frequency) resolution as the WT [32].Moreover, unlike other fixed resolution JTFA techniques, the WT allows a variable resolution and facilitates better time resolution of high frequencies and better frequency resolution of lower frequencies. Although wavelet analysis has often been quoted as the panacea for analyzing non-stationary signals (and thereby overcoming the problem of the Fourier transform, which assumes stationary), it is sometimes important to segment data at non-stationary. An example of such a situation may be a sudden change in dynamics that requires a change in the chosen analysis technique. Of course, JTFA may aid in defining a point of segmentation.

In the following section, brief overviews of some of the key concepts in wavelet denoising are presented from the beginning of Fourier transform.

5.3.1 Fourier Transform

The most well-known of these is Fourier analysis, which breaks down a signal into constituent sinusoids of different frequencies. Another way to think of Fourier analysis is as a mathematical technique for transforming our view of the signal from a time-based one to a frequency-based one like Fig 5.4.

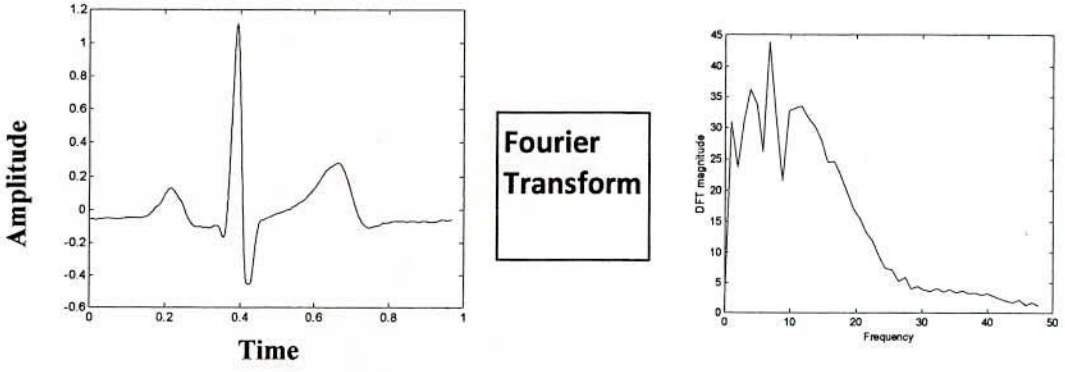

Figure 5.4 : Fourier transform of a signal.

For many signals, Fourier analysis is extremely useful because the signal's frequency content is of great importance. Fourier analysis has a serious drawback while transforming to the frequency domain, time information is lost. When looking at a Fourier transform of a signal, it is impossible to tell when a particular event took place. If a signal doesn't change much over time — that is, if it is what is called a stationary signal — this drawback isn't very important [33]. However, most interesting signals contain numerous non-stationary or transitory characteristics: drift, trends, abrupt changes, and beginnings and ends of events like ECG . These characteristics are often the most important part of the signal and Fourier analysis is not suited to detecting them.

5.3.2 Short -Time Fourier Transform

In an effort to correct this deficiency, Dennis Gabor (1946) adapted the Fourier transform to analyze only a small section of the signal at a time — a technique called windowing the signal. Gabor's adaptation, called the Short-Time Fourier Transform (STFT), maps a signal into a two-dimensional function of time and frequency like Fig 5.5.

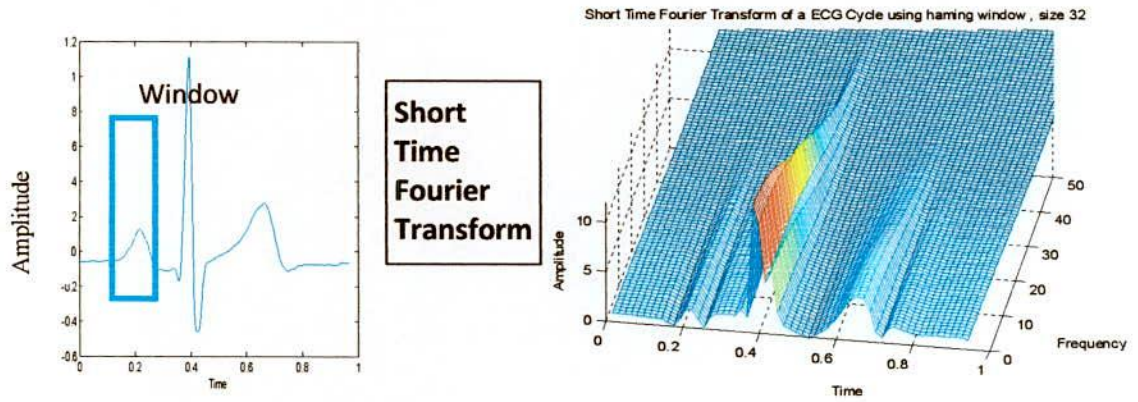

Figure 5.5: Short time Fourier transform of a signal.

The STFT represents a sort of compromise between the time- and frequency-based views of a signal. It provides some information about both when and at what frequencies a signal event occurs. However, we can only obtain this information with limited precision, and that precision is determined by the size of the window [33].

While the STFT's compromise between time and frequency information can be useful, the drawback is that once we choose a particular size for the time window, that window is the same for all frequencies. Many signals require a more flexible approach — one where we can vary the window size to determine more accurately either in time or frequency. But it is desired that since the frequency of a signal is directly proportional to the length of its cycle, it follows that for high-frequency spectral information, the time-interval should be relatively small to give better accuracy and for low-frequency spectral information, the time-interval should be relatively wide to give complete information. In other words, it is important to have a flexible time-frequency window that automatically narrows at high "'center-frequency" and widens at low "center-frequency". Fortunately, Wavelet analysis represents the next logical step: a windowing technique with variable-sized regions. Wavelet analysis allows the use of long time intervals where we want more precise low frequency information, and shorter regions where we want high frequency information.

5.3.3 Continuous Wavelet Transform

Literally "wavelet" means "a small wave". Mathematically it is a function that has finite energy and zero mean. It is derived from short window Fourier transforms (STFT) whose main characteristics are the multiresolution, consisting an accepted way for the analysis of transient, nonstationary characteristics Such as drift, trends, abrupt changes, beginning and

end of events, breakdown points and discontinuities in higher derivatives and self similarity as bioelectrical signals are.

Here's what this looks like in contrast with the time-based, frequency-based and time-frequency based views of a signal as represented in Fig 5.6 [33] [34]:

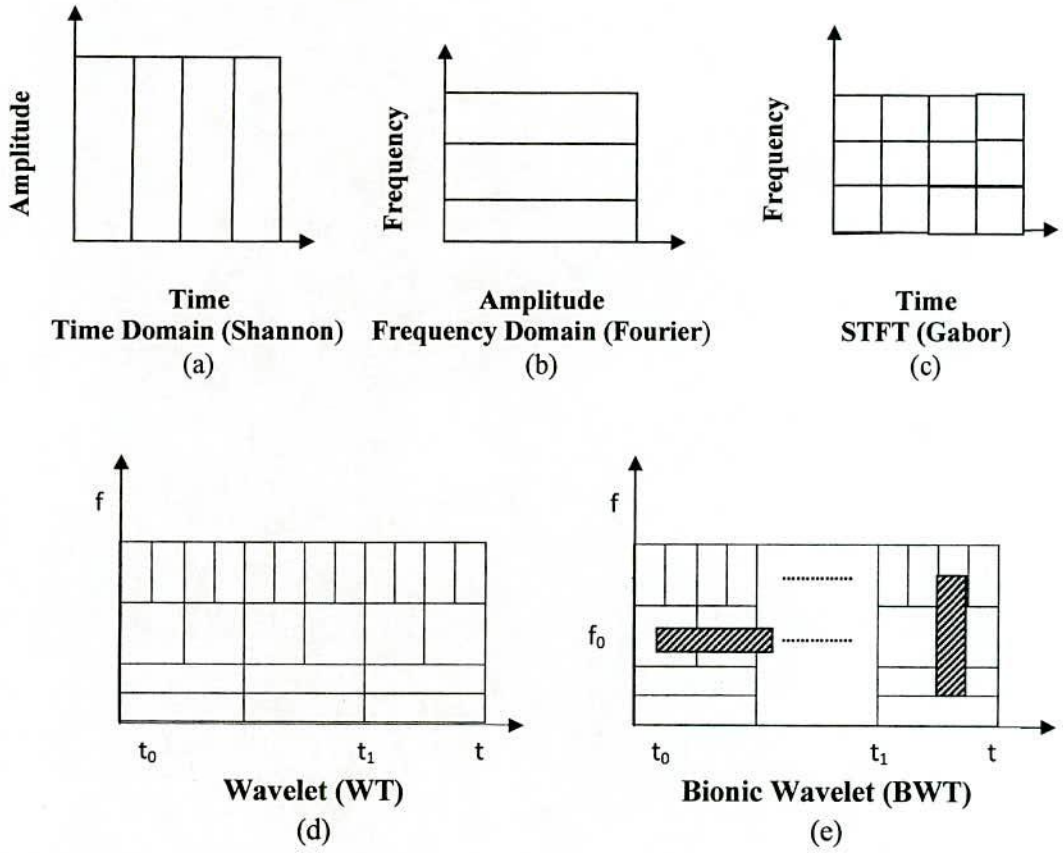

Figure 5.6: Different types of plane represented by (a) Time domain ,(b) Frequency domain,(c) Time-frequency (STFT) domain (d) time–frequency resolutions by WT (e) time–frequency resolutions by BWT. The window-widths along the time and frequency axis represent the time and frequency resolutions of TFR, respectively. The shadowed and blank windows represent the time–frequency resolutions of BWT and WT, respectively.

The wavelet analysis is one way to localize events in time (or space) and frequency. The goal of wavelet analysis is to create a self-of basis functions (i.e, expansion function) so that transform will give an informative, efficient and useful description of the target signal. In a nutshell, the continuous wavelet (CWT) is nothing but a set of the inner product of the observed signal $f(t)$ with the shifted and scaled mother wavelets $\psi_{a,\tau}(t)=\frac{1}{\sqrt{a}}\psi(\frac{t-\tau}{a})$ where τ and a >0 represent the time shift and scale variable respectively.

$$< f(t), \psi_{a,\tau} > WT_f(a,\tau) = \frac{1}{\sqrt{a}} \int f(t)\psi^* \left(\frac{t-\tau}{a}\right) dt \tag{5.10}$$

It is noted that any function cannot be treated as a mother wavelet. Only those functions can be treated as mother wavelet function which can satisfy the admissible condition of wavelet [35].

Like STFT, a wavelet transform can represent the time frequency variation of the spectral components, but it has a different time frequency resolution which can correlate f with $\psi_{a,\tau}$ by applying the Fourier Parseval formula, it can be written as integration of frequency [36].

$$Wf(a,\tau) = \int_{-\infty}^{\infty} f(t)\psi^*_{a,\tau}(t)dt = \frac{1}{2\pi}\int_{-\infty}^{\infty} \hat{f}(\omega)\,\hat{\psi}_{a,\tau(\omega)}d\omega \tag{5.11}$$

The wavelet coefficient $Wf(a,\tau)$ thus depends on the values of f(t) and $\hat{f}(\omega)$ in the time-frequency region where the energy of $\psi_{a,\tau}$ and $\psi^*_{a,\tau}$ is concentrated. Time-varying harmonics are detected from the position and scale of the high amplitude wavelet coefficient.

In time $\psi_{a,\tau}$is centered at τ with spread proportional to a and its Fourier transform is calculated from [36].

$$\hat{\psi}_{a,\tau(\omega)} = e^{-i\tau\omega}\sqrt{a}\hat{\psi}(a\omega) \tag{5.12}$$

Where $\hat{\psi}$ is the Fourier transform of ψ. The time and frequency spread are respectively proportional to a and $\frac{1}{a}$. That means lower scale represents the higher frequency (rapidly changing details) and higher scale represent the opposite phenomena. Easily it can be demonstrated that pseudo frequency of any scale easily determined by $f_a = \frac{f_c}{a.\Delta}$, where Δ is

the sampling period. In this way we can represent the time scale wavelet transform to time-frequency representation.

Then the ratio of the center-frequency to the width of the frequency band is (called Q-factor) given by $\frac{\omega^*/a}{2\Delta_{\psi}/a} = \frac{\omega^*}{2\Delta_{\psi}}$,which is independent of the location of the center-frequency. This is called "constant-Q" frequency analysis [37]. The importance of the time-frequency window is that it narrows for large center-frequency ω^*/a_2 and widens for small center-frequency ω^*/a_1 shown in Fig 5.7.

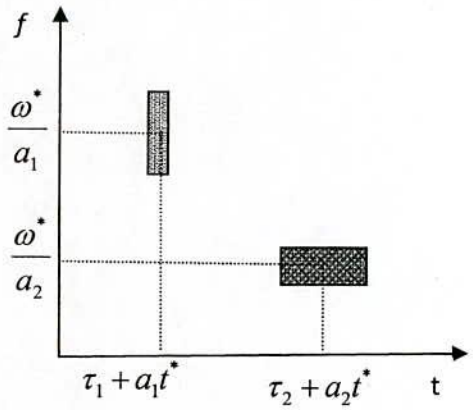

Figure 5.7: Understanding constant–Q filtering of wavelet in the time-frequency plane.

5.3.4 Discrete Wavelet Transform (DWT)

As CWT is much redundant representation, it can be described by setting $a = a_0^i$ and $\tau = k\tau_0 a_0^i$with i and k are integers and a_0 is real valued greater or equal 1. A practical choice of τ_0 and a_0 consists on setting a_0 to 2 and τ_0 to 1 that is $a = 2^i$ and $\tau = k2^i$ which is dyadic or octave wavelet transform [35].

$$\psi_{i,k}(t) = 2^{-\frac{i}{2}}\psi(2^{-i}t - k) \tag{5.13}$$

So for a given signal $f(t)$,the DWT decomposition can be represent by

$$f(t) = \sum_{k=-\infty}^{\infty} a_{N,K}\varphi(2^{-N}t - K) + \sum_{j=1}^{\infty}\sum_{k=-\infty}^{\infty} d_{j,k}2^{-\frac{j}{2}}\psi\,(2^{-j}t - K) \tag{5.14}$$

Where $a_{N,K}$ represents approximate coefficients of level N while d(j=1,2,……..N) represent detailed coefficient or wavelet coefficient at level j. $\psi(t)$ is the wavelet while φ(t) is a companion function, named scaling function.

The DWT consists of applying the discrete signal to a bank of octave band filters based on low and high pass filters $h(n)$ and $g(n)$ respectively. More precisely, the function $f(t)$ would be expressed as signal expression point of view like

$$f(t) = \sum_{k \in Z} a_L(k)\, \varphi_{L,k}(t) + \sum_{j=1}^{L} \sum_{k \in Z} d_j(k)\, \psi_{j,k}(t) \tag{5.15}$$

Now if we relate the above equation with filter bank point of view then [38]

$$d_j(n) = < f, \psi_{j,n} > = \frac{1}{\sqrt{2}} \sum_{k} g(2n-k)\, a_{j-1}(n) \tag{5.16}$$

$$a_L(n) = < f, \varphi_{j,n} > = \frac{1}{\sqrt{2}} \sum_{k} h(2n-k)\, a_{L-1}(n) \tag{5.17}$$

Where $\varphi(t)$ is called scaling function associated to the wavelet function $\psi(t)$ goverened by the following condition $\int \varphi(t)dt = 1$, $h(n)$ and $g(n)$ are the low pass and high pass filter of the filter bank. A 3-level decomposition of orthogonal wavelet basis is illustrated in Fig.5.8, that is, detail coefficients at all the three levels (D_1, D_2, and D_3) and approximate at deepest decomposition level (A_3). Approximate coefficients often resemble the signal itself.

Now for calculating approximation and details, we need to know the coefficient of low pass $h(n)$ and high pass $g(n)$ .In the following section wavelet decomposition is performed using Daubechies wavelet of length 4 and 6.

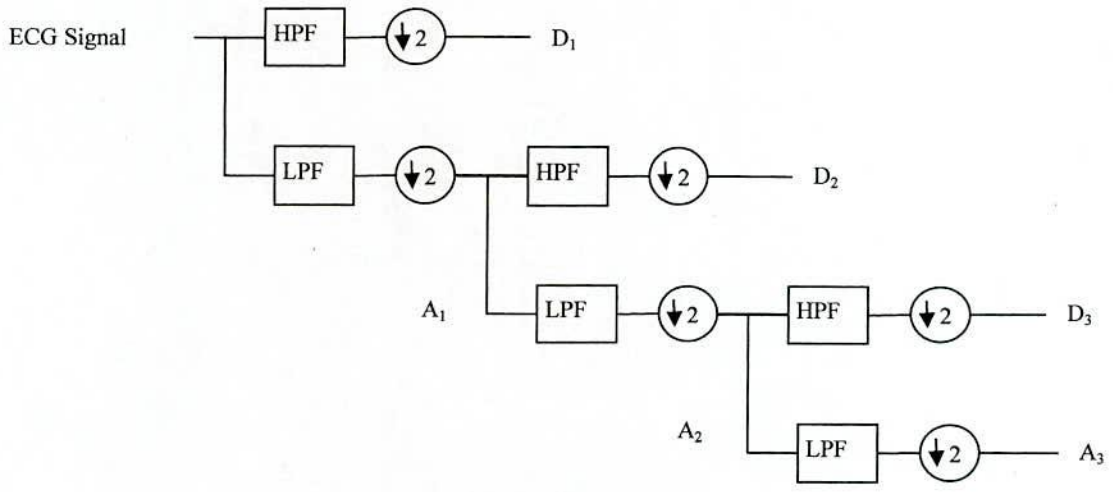

(a) Decomposition

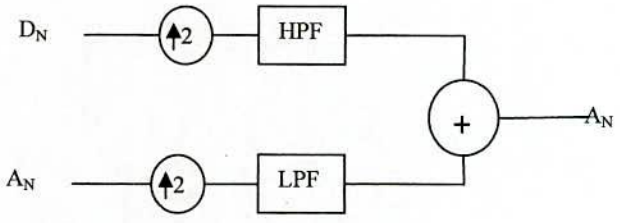

(b) Reconstruction

Figure 5.8. Wavelet decomposition and reconstruction filter model.

5.3.4.1 Daubechies wavelet

The Daubechies wavelet are the family of orthogonal wavelet defining a discrete wavelet transform and characterized by a maximal number of vanishing moments for some given support. With each wavelet type of this class, there is a scaling function which generates an orthogonal multiresolution analysis [38]. It is one of the brightest wavelet on research which is compactly supported.

D-4 means low pass and high pass filter coefficient has 4 coefficients each which obey orthogonality condition of the wavelet.

This two equations show that, the scaling and wavelet coefficients at different levels of scale can be obtained by convolving the expansion coefficient at scale j by the time-reversed and down sampling (shown in the matrix) [39]. For calculating $h(n)$ and $g(n)$,we use a complementary derivation of Daubechies wavelet using an orthogonal transformation matrix, W_8 in block format

$$W_8 = \left[\begin{array}{cccccccc} h_3 & h_2 & h_1 & h_0 & 0 & 0 & 0 & 0 \\ 0 & 0 & h_3 & h_2 & h_1 & h_0 & 0 & 0 \\ 0 & 0 & 0 & 0 & h_3 & h_2 & h_1 & h_0 \\ h_1 & h_0 & 0 & 0 & 0 & 0 & h_3 & h_2 \\ \hline g_3 & g_2 & g_1 & g_0 & 0 & 0 & 0 & 0 \\ 0 & 0 & g_3 & g_2 & g_1 & g_0 & 0 & 0 \\ 0 & 0 & 0 & 0 & g_3 & g_2 & g_1 & g_0 \\ g_1 & g_0 & 0 & 0 & 0 & 0 & g_3 & g_2 \end{array}\right] = \left[\frac{H}{G}\right] \tag{5.18}$$

Where H denotes upper matrix and G denotes the lower matrix. Now computing $W_8 W_8^T$ and insisting that W_8 is orthogonal gives that

$$W_8 W_8^T = \left[\frac{H}{G}\right]\left[H^T \middle| G^T\right] = \left[\frac{HH^T}{GH^T}\middle|\frac{HG^T}{GG^T}\right] = \left[\frac{I_4}{0_4}\middle|\frac{0_4}{I_4}\right] \tag{5.19}$$

where I_4 is 4×4 identity matrix and 0_4 is 4×4 zero matrix. Lets analyze and calculating HH^T from above, we get

$$\mathrm{I}_4 = HH^T = \begin{bmatrix} \mathrm{c} & \mathrm{d} & 0 & \mathrm{d} \\ \mathrm{d} & \mathrm{c} & \mathrm{d} & 0 \\ 0 & \mathrm{d} & \mathrm{c} & \mathrm{d} \\ \mathrm{d} & 0 & \mathrm{d} & \mathrm{c} \end{bmatrix} = \begin{bmatrix} 1 & 0 & 0 & 0 \\ 0 & 1 & 0 & 0 \\ 0 & 0 & 1 & 0 \\ 0 & 0 & 0 & 1 \end{bmatrix} \tag{5.20}$$

where $c= h_0^2 + h_1^2 + h_2^2 + h_3^2$ and $d=h_0h_2+h_1h_3$ and by definition of orthogonality $c=1$ and $d=0$.

Now we get $h_0^2 + h_1^2 + h_2^2 + h_3^2 = 1$ (5.21)

$h_0h_2+h_1h_3 = 0$ (5.22)

If we analyze HG^T and GH^T, it becomes zero and GG^T is same as HH^T.

As $h(n)$ is low pass filter coefficient and we need four equation to get the four filter coefficient for D-4. By imposing on $h(n)$ using Fourier series

$H(\omega) = h_o + h_1 e^{iw} + h_2 e^{2iw} + h_3 e^{3iw}$ and for low pass $H(0)=1$ and $H(\pi)=0$.

We get $H(0) = h_o + h_1 + h_2 + h_3 = 1$ (5.23)

and $H(\pi) = h_o - h_1 - h_2 - h_3 = 0$ (5.24)

But it can be proved that to maintain orthogonality $|H(0)| = \sqrt{2}$.

$$i.e. |H(0)| = |h_o + h_1 + h_2 + h_3| = \sqrt{2} \quad (5.25)$$

An additional low pass condition $H'(\pi) = 0$, where differentiation form of $H(\omega)$ is $H'(\omega)$

So we get $h_1 - 2h_2 + 3h_3 = 0$ (5.26)

Finally the system equation of $h(n)$ of *D-4 is*

$$\left.\begin{array}{c} h_0^2 + h_1^2 + h_2^2 + h_3^2 = 1 \\ h_o h_2 + h_1 h_3 = 0 \\ h_0 - h_1 - h_2 - h_3 = 0 \\ h_1 - 2h_2 + 3h_3 = 0 \end{array}\right\} \quad (5.27)$$

Solving this equation we can find

$$h_0 = \frac{(1+\sqrt{3})}{4\sqrt{2}}, \quad h_1 = \frac{(3+\sqrt{3})}{4\sqrt{2}}, h_2 = \frac{(3-\sqrt{3})}{4\sqrt{2}}, h_3 = \frac{(1-\sqrt{3})}{4\sqrt{2}}$$

And it maintain the orthogonality condition . From high pass filter coefficient $g(n)$ can easily be calculate from $h(n)$ using the following equation.

$g_k = (-1)^k h_{L-k}$ *for* $k=0,1,2,....,(L-1)$ (5.28)

where L is the length or order of the filter. So $g_0 = h_3, g_1 = -h_2, g_2 = h_1, g_3 = -h_0$

Using the above procedure and equating $H^{(m)}(\pi)=0$, where m the number of differentiation, $m=0,1,\ldots,\frac{L-1}{2}$,we get the coefficient of D-6 and D-8 shown in table 5.1 [36].

Table 5.1: coefficient of Db-6 and Db-8.

n	Db-6 coefficient of h_n	*Db-8 coefficient of h_n*
0	0.332671	0.2303778
1	0.806 892	0.7148466
2	0.459878	0.6308808
3	-0.135011	-0.0279838
4	-0.085441	-0.1870348
5	0.035226	0.03084138
6		0.03288301
7		-0.0105974

Other wavelet coefficients are discussed in appendix I. In this research, Daubechies, Coiflet and symlet wavelet is used since its scaling and wavelet function is closely related to the shape of ECG [75](shown in Fig 5.9.) and suited for denoising for many applications.

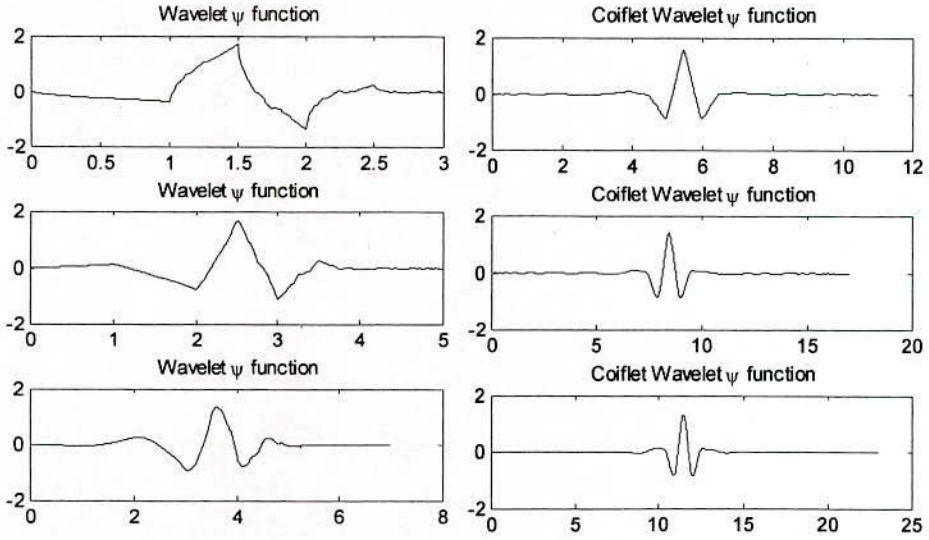

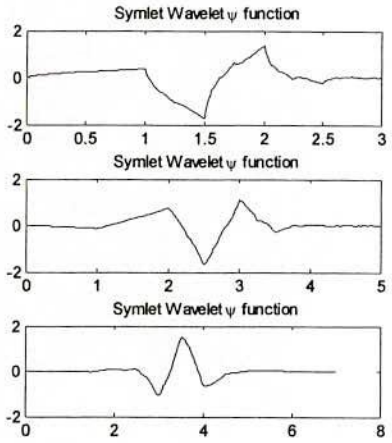

(c)

Figure 5.9: Different types of mother wavelet (a) Daubachies (b) Coiflet (c) Symlet.

5.4 Tunable-Q Wavelet Transform (TQWT)

As demonstrated earlier that, the traditional wavelet transform has constant quality factor Q. But it is not so efficient for all types of signal. Q-factor should be tuned according to the oscillatory behavior of the signal to which it is applied. For example, when using wavelets for the analysis and processing of oscillatory signals (speech, ECG, EEG, etc), the wavelet transform should have a relatively high Q-factor. But the Q-factor of the conventional wavelet transform is constant and low. It needed higher Q for oscillatory signals (speech, ECG, EEG, etc).

Recently Ivan W. Selesnick proposed Wavelet Transform With tunable Q-factor called the tunable-Q wavelet transform (TQWT) [40]. This is parameterized by its Q-factor and its oversampling rate (redundancy). The TQWT is developed using perfect reconstruction over-sampled filter banks with real-valued scaling factors. The TQWT is closely related to the rational-dilation wavelet transform (RADWT) [41]. Like the RADWT, the TQWT is fully discrete, has the perfect reconstruction property, is modestly over complete, is developed in terms of iterated two-channel filter banks and implemented using the DFT. In contrast to the RADWT, the TQWT is simpler conceptually, can be more efficiently implemented using radix-2 FFTs and its parameters are more easily related to the Q-factor of the transform. The user can directly specify the Q-factor and redundancy of the TQWT

[40]. The tunability of TQWT is achieved by low-pass scaling with scaling parameter α and high-pass scaling with scaling parameter β.

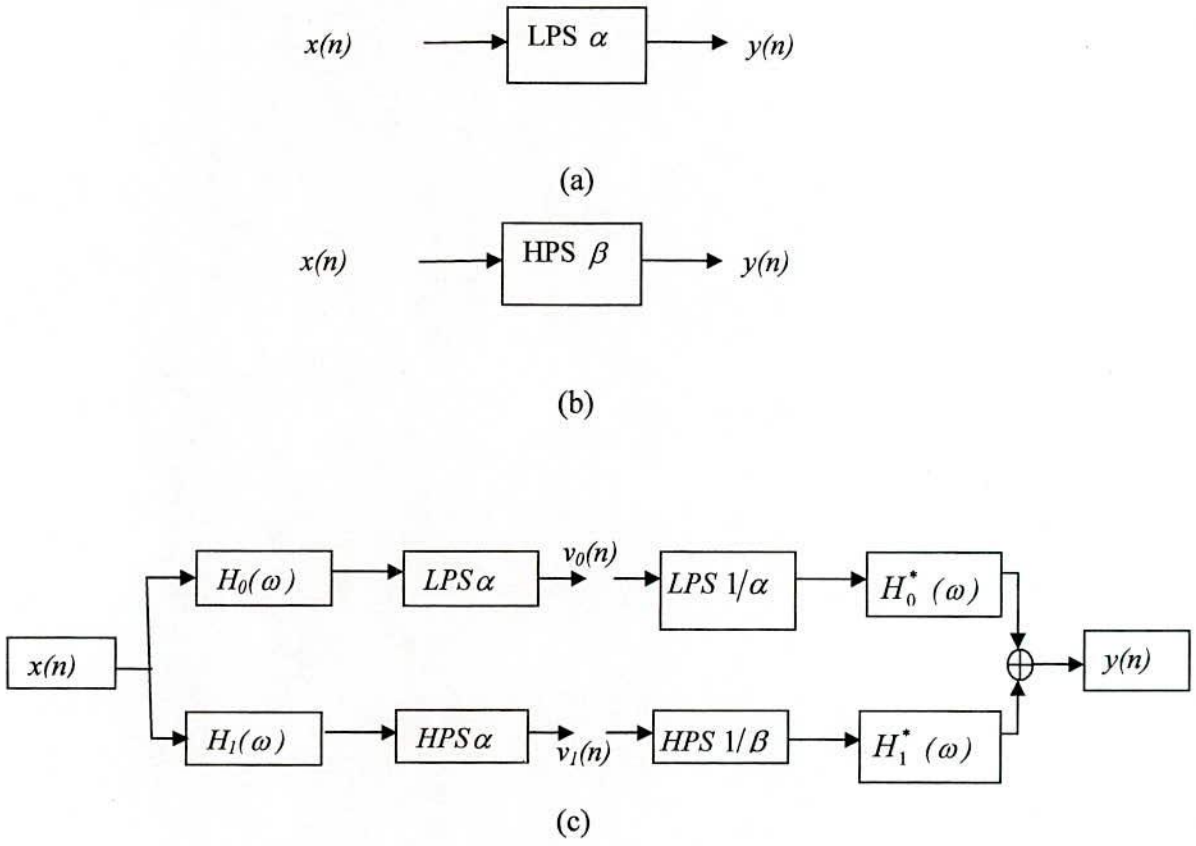

Figure 5.10: (a) Low-pass scaling block diagram , (b) High-pass scaling block diagram. Analysis and synthesis filter banks for the tunable-Q wavelet transform. The subband signal $v_0(n)$ has a sampling rate of αf_s where f_s is the sampling rate of the input signal $x(n)$. Likewise, the subband signal $v_1(n)$ has a sampling rate of βf_s. LPS and HPS represent low-pass scaling and high-pass scaling respectively.

Oversampling rate (redundancy): The two-channel filter bank illustrated in Fig. 5.10 is oversampled by a factor of $\alpha + \beta$. If the two-channel filter bank is iterated on its low-pass output at infinitum so as to implement a wavelet transform, then the wavelet transform is oversampled by a factor of

$$r = \frac{\beta}{1-\alpha} \tag{5.29}$$

which we call the redundancy r of the wavelet transform [40]. This expression is obtained by noting that the sampling rate at subband j (with $j \geq 1$) is given by $\beta\alpha^{j-1}f_s$, where f_s is the sampling rate of the input signal. The sum of the sampling rates over all subbands $j \geq 1$ gives $\frac{\beta}{1-\alpha}.f_s$ and hence the oversampling rate in (5.29).

Center frequency: The center frequency at level-j frequency response, in the interval (ω_1, ω_2) given by

$$\omega_c = \frac{1}{2}(\omega_1 + \omega_2) = \alpha^j \frac{2-\beta}{2\alpha}\pi \tag{5.30}$$

In terms of the input signal sampling rate f_s , the center frequency at level j is $f_c = \alpha^j \frac{2-\beta}{4\alpha} f_s$ .The bandwidth is given by $BW = \frac{1}{2}(\omega_1 - \omega_2) = \frac{1}{2}\beta\alpha^{j-1}\pi$. The Q-factor can be given by $Q = \frac{\omega_c}{BW} = \frac{2-\beta}{\beta}$ .Note that the Q-factor does not depend on the level j. As expected, the wavelet transform is a constant-Q transform [40]. The filter bank parameters α, β can be chosen to achieve a wavelet transform with the desired Q-factor and oversampling rate r by the following equation.

$$\beta = \frac{2}{Q+1} \text{ and } \alpha = 1 - \frac{\beta}{r} \tag{5.31}$$

This is brief description about TQWT. More information can be get at [42].

5.5 Proposed Discrete Bionic Wavelet Transform

Due to different oscillating behavior of signal , constant Q of wavelet is not as effective as variable Q. The variable Q is changed with the instantaneous value of a signal and it will make Bionic wavelet more adaptive compared to TQWT. Because in TQWT, Q-factor is tuned to a fixed value, but in variable Q-wavelet transform like Discrete Bionic Wavelet transforms (DBWT) which is the discrete version of BWT, Q is changed with the

instantaneous value of a signal and its first order difference. This adaptive quality factor Q is derived from the active biological model of heart.

Very few works were done in the past several years on BWT. To the best of our knowledge, only BWT based on the active auditory model of cochlea was introduced by [4] and used in the speech signal processing. This model is not appropriate for biomedical signal processing like ECG. Furthermore, it is very hard to know what entropy function is used in the bio-system. This is a problem of other transforms. But, the DBWT uses active control mechanism of heart-arterial system to adjust the wavelet function rather than entropy function as criterion.

5.5.1 Derivation of *T*-function

Since William Harvey established the concept of circulation of blood in 1628, numerous attempts have been made at gaining insight into the physical relationship between the forces involved in propelling blood in the complicated anatomical structure of the circulatory system. If we consider for a moment that the concept of the blood circulation in human body, we can imagine that we have a pump delivering blood to a complicated network of pipes, which has innumerable connections. To develop an adequate mathematical model of this system and its behavior is an almost impossible task. Thus in Oder to make progress, we call "heart-arterial interaction model" which is shown in Fig.5.11 (a). Here A and B represents the proximal(very near to heart) and distal (away from the heart) location. The proximal and distal part can be modeled by lumped parameter model. In this model distal part can be modeled by three element windkessel model as shown in Fig. 5.11(b). This model mainly consists of six components. An *AC* power supply $P_v(t)$, a diode D, two impedance components (z_0, Rs) and a capacitance C(p). The diode D represents the unidirectional flow and Q *(t)* is the overall blood flow rate. In Physiological terms, $P_v(t)$ is the time varying pressure source depending on time *t*, ventricular volume V_v, outflow Q_v , Aortic valve *D*. R_v= systolic ventricular resistance, z_o= aortic characteristic impedance, R =total peripheral resistance , $C(p)$= pressure dependent dynamic arterial compliance. $P_a(t)$ and $Q(t)$ are aortic pressure and flow respectively.

This heart-arterial interaction model was used to derive the *T*-function where heart can be described as pressure source [43] [44]. The electrical analog of the system can be represented by lumped-parameter model and is shown in Fig 5.11.

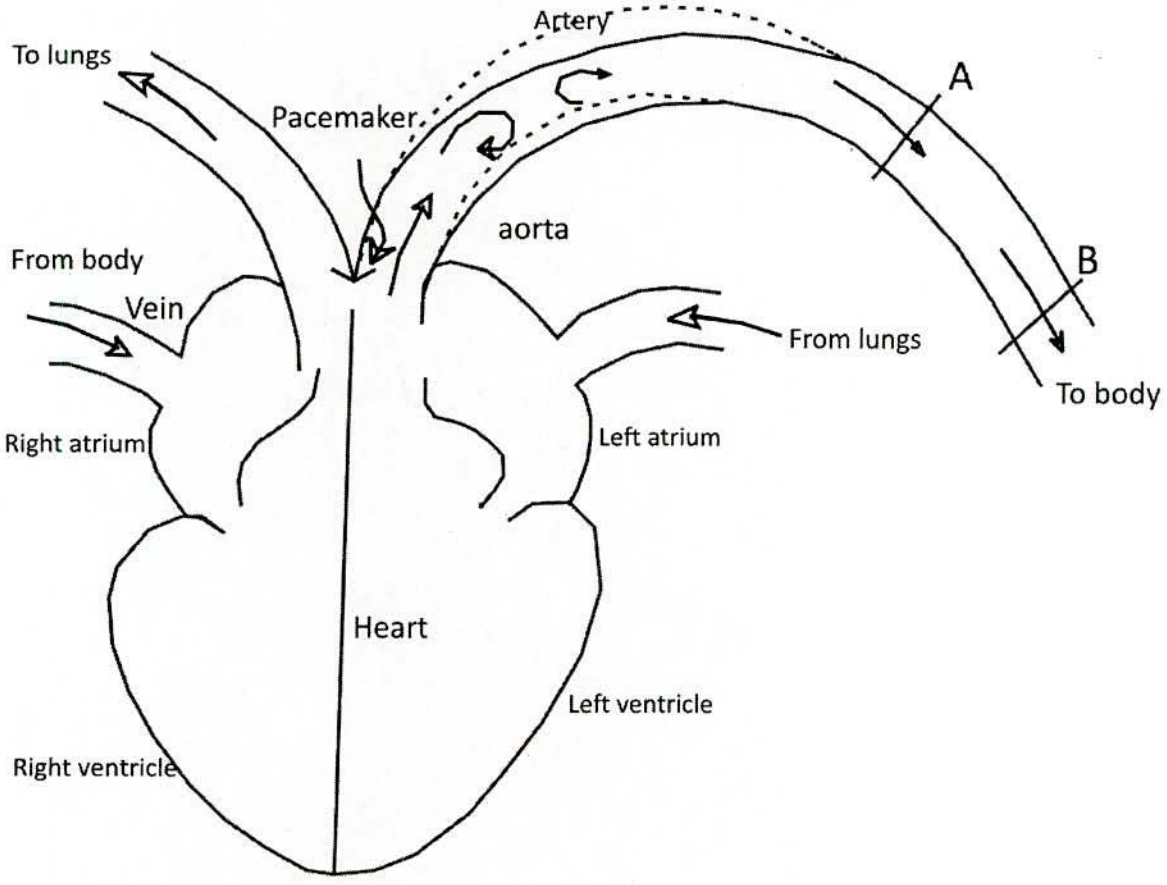

(a)

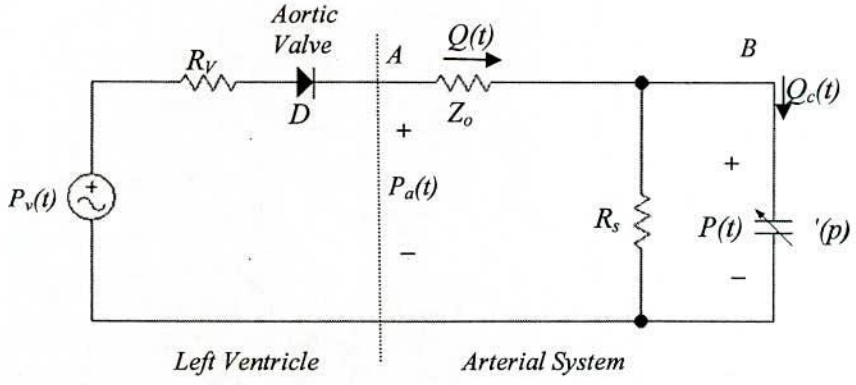

Figure 5.11: (a) A schematic figure of human heart and the arterial system. (b) Electrical Analog of modified heart-arterial system proposed by the present study.

In the true sense, the arterial wall are geometrically tapering, viscoelastic and follow the Womersley's oscillatory flow theory. And the pressure transfer function relates the distal pressure wave (P_{distal}) to the proximal pressure wave ($P_{proximal}$), with reflection coefficient Γ and propagation coefficient γ with length L as [45] Here distal pressure means the pressure away from, farther from the heart and proximal pressure means the pressure Near, closer to the heart.

$$T = \frac{P_{distal}}{P_{proximal}} = \frac{e^{-\gamma z} + \Gamma e^{-\gamma L}}{1 + \Gamma e^{-2\gamma z}} = \frac{(1+\Gamma)e^{-\gamma z}}{1 + \Gamma e^{-2\gamma z}} \tag{5.32}$$

The propagation coefficient is $\gamma = \frac{\omega}{c_o}\frac{\sqrt{1-\sigma^2}}{\sqrt{1-F_{10}}}e^{-j\theta/2}$ (5.33)

Where ω is angular frequency= $2\pi f$, f is the frequency of the heart, c_o is the wave velocity calculated by the Moens-Korteweg, σ is the Poisson ration of the wall material, F_{10} is the Womersley's function describing the fluid flow in the tube and θ is the wall viscosity as a function of frequency, $\theta = \theta_0(1 - e^{-2\omega})$ [46] For details of this transfer function see Appendix II.

But the T-function derived from tapering, Womersley's and viscoelastic tube is difficult. A single uniform lossless tube with three element windkessel load is sufficient to describe the model and easy also [47]. Three element windkessel model has been chosen in this study because the classical two-element model (the windkessel) accounts for the lowest frequency components, and the three-element model (the modified windkessel) accounts for both low- and high-frequency components of the spectrum of interest [48].

The incident (forward) pressure wave travel along the tube with time delay , but with no deformation until it reaches the end of the tube (Fig 5.12). At that point, the pressure wave reflect backward according to the reflection coefficient (Γ) which arises from the mismatch between the characteristic impedance of the tube and terminal impedance [49].

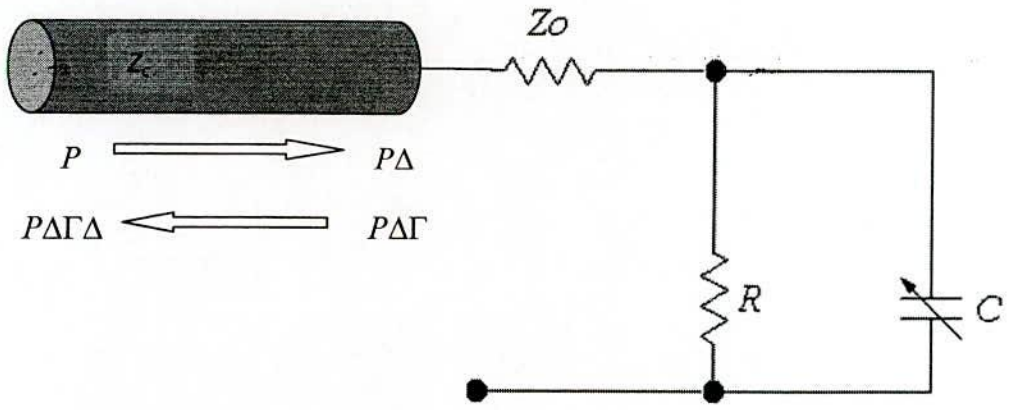

Figure 5.12: Schematic representation of the arterial model which consists of a pure elastic lossless tube terminated with a modified Windkessel model.

The reflected backward wave, now travel with the same time delay Δt with no deformation, but towards the aortic root. The sum of this forward and backward pressure wave forms the actual pressures at the periphery to aorta [49] [50].

So the transfer function is $T(\omega)=\dfrac{P\Delta+P\Delta\Gamma}{P+\Delta\Gamma\Delta}=\dfrac{Pe^{-j\omega\Delta t}+Pe^{-j\omega\Delta t}\Gamma}{P+Pe^{-j\omega\Delta t}\Gamma e^{-j\omega\Delta t}}=\dfrac{(1+\Gamma)e^{-j\omega\Delta t}}{(1+\Gamma e^{-2j\omega\Delta t})}$ (5.34)

If we express the impedance of the terminating arterial system as z, the reflection coefficient, Γ is expressed as $(z-z_c)/(z-z_c)$.Since the hydraulic pressure and flow rate are analogous to electrical voltage and current respectively, this can represent the electrical event of the heart as in [51].

5.5.2 Derivation of Proposed Discrete Bionic Wavelet Transform (DBWT)

If the constant Q_o is the quality factor of WT, then the quality factor Q_T of BWT is related to Q_o by [4]:

$$Q_T = TQ_o . \quad (5.35)$$

Where T-function is the modified from the heart-arterial model for Discrete Bionic Wavelet as

$$T = \frac{(1 + X_{DBWT})e^{-j\omega\Delta t}}{(1 + G_1 \times X_{DBWT} e^{-2j\omega\Delta t})} \tag{5.36}$$

Only negative damping is not enough to describe all the functions of heart. we introduce second term into the function of T as imposed in [52].

$$T = \frac{(1 + X_{DBWT})e^{-j\omega\Delta t}}{(1 + G_1 \times X_{DBWT} e^{-2j\omega\Delta t})} \times \frac{1}{\left(1 + G_2 \times \left|\frac{\partial}{\partial \tau} X_{DBWT}\right|\right)} \tag{5.37}$$

Where j the imaginary unit, and ω is the angular frequency, i.e., $2\pi f$ with f heart frequency.G_1 and G_2 are the saturation factor. The value of G_1 and G_2 are taken where the highest value of SNR improvement and heart frequency is normally *1.2 Hz*. In our research they are 2 and 0.23 respectively. According to model-3 of [53] Δt can be set as 0.048.

First DWT of the noisy ECG is taken then the time adaptive nature is captured by time varying factor $T(a,\tau))$, calculation for each scale ($a = 2^m$) and time ($\tau = n\,2^m$) using eqn. 5.37. This factor only affects the duration of amplitude envelope of wavelet, but not affects the frequency. Since, the primary adaptation mechanism involves variation of the wavelet time support, the impact of initial time support was done by turning off adaptation mechanism ($T(a,\tau)$=1). The resulting time adaptive wavelet transform coefficients $X_{DBWT}(a,\tau)$ are calculated from the product of DWT, $X_{DWT}(a,\tau)$ with a time constant $K(a,\tau)$ and the same is substituted in eqn. 5.37 for time adaptation mechanism. It can be write as [54].

$$X_{DBWT} = K(a,\tau) \times X_{DWT}(a,\tau) \tag{5.38}$$

$$K(a,\tau) = \frac{\sqrt{\pi}}{C} \cdot \frac{1}{\sqrt{1 + T^2(a,\tau)}} \tag{5.39}$$

where $C_0 + C_1 + C_2 + ... + C_7 = 2$ (normalizing constant).

The normality is obtained by $C(n) = \sqrt{2}\ h(n)$.

5.6 Thresholding Algorithm

Denoising by wavelet is performed by thresholding algorithm, in which coefficients smaller than a specific value, or threshold, will be shrunk or scaled [55] [56]. In this section, we review some of the most used thresholding algorithms. In these algorithms, the variable x refers to wavelet coefficients indices and Th is the threshold value.

5.6.1 Hard Thresholding Algorithm

Hard thresholding is similar to setting the components of the noise subspace to zero. Donoho and Johnstone used it in [57] for wavelet thresholding as:

$$\delta_T^H(x) = \begin{cases} 0 & |x| \leq Th \\ x & |x| > Th \end{cases} \tag{5.40}$$

In this thresholding algorithm, the wavelet coefficients less than the threshold Th will be replaced with zero, as Fig 5.13(a) represents.

5.6.2 Soft Thresholding Algorithm

In which, thresholding algorithm is defined as follow [57] (see Fig 5.13(b))

$$\delta_T^H(x) = \begin{cases} 0 & |x| \leq Th \\ sign(x)(|x| - Th) & |x| > Th \end{cases} \tag{5.41}$$

which can be viewed as setting the components of the noise subspace to zero, and performing a magnitude subtraction in the ECG plus noise subspace.

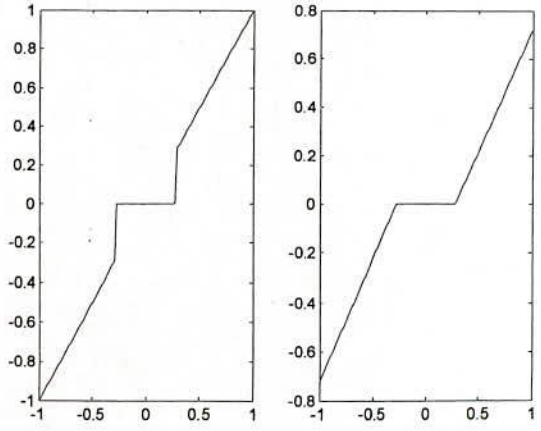

(a) (b)

Figure 5.13: Hard thresholding and Soft thresholding.

5.7 Threshold Selection

There are also many formulas for obtaining threshold values. In this section we review some of the most popular of them. In all these formulas *Th* is the threshold value.

5.7.1 Universal Method

Donoho and Johnstone derived a general optimal universal threshold for the white Gaussian noise under a mean square error criterion and its side condition [57]. In this method threshold is selected as:

$$Th = \hat{\sigma}\sqrt{2\log_e(n)} \tag{5.42}$$

In this formula n is number of samples in the noisy signal and r is the standard deviation of noise that is estimated by the relation [58]:

$$\hat{\sigma} = \left[\frac{median(|Y_{ij}|)}{0.6745}\right] \tag{5.43}$$

In which $|Y_{ij}|$ is the first level detail coefficients of wavelet transform of noisy ECG. This selection for *Th* is based on a theorem that if $Z_i = N(0, 1)$ then

$$prob\{||z_i||_{i_n^\infty} \leq \sqrt{2\log n}\} \to 1 \tag{5.44}$$

In this relation $||$ is the Norm operator and l^k is the k^{th} risk function.

$$(.)_{l^k} = E\left(\overset{K}{.}\right) \tag{5.45}$$

Therefore, if $Z_i = N(0,d)$ then a good estimate for *Th* is as (5.42) [56].

In practice the threshold obtained by this method is not ideal for ECG signals due the poor correlation between MSE and subjective quality and the more realistic presence of correlated noise [59].

5.7.2 Heuristic Method

Heuristic variant of the rigorous sure method is called Heuristic Sure. It is the synthesis of two thresholds and the optimal selection of predictor variable threshold. If the SNR is small(estimated to be a great noise), we use this heuristic threshold in this case [33].

5.7.3 Minimax Method

In this method, also proposed by Donoho and Johnstone, it supposed that $X = N(\theta, 1)$ is the observation value; then Th is selected in a way that minimizes the following relation:

$$\Lambda_n^* = \inf_{\text{Th}} \sup_{\theta} \left\{ \frac{E(\sigma_{Th}(X)-\theta)^2}{n^{-1}+\min(\theta^2,1)} \right\} \tag{5.46}$$

Here, $\delta_{Th}(X)$ is the shrink function or thresholding algorithm and n is number of signal samples.

5.7.4 SURE Method

SURE or stein unbiased risk is also introduced by Donoho and Johnstone as:

$$SURE(Th; w) = \frac{\sigma^2}{2^j} + \frac{\sigma^2}{n} \sum_{j=1}^{J} \sum_{k} S_{Th_j} \left(\frac{d_{j,k}}{\sigma} \right) \tag{5.47}$$

In this formula n is number of signal samples, J is number of levels in wavelet decomposition, K is number of samples in the level and σ is the standard deviation of noise. $S_{Th}(x)$,which is determined with due attention to $\delta_{Th}(X)$, must be such that:

$$E\{S_{Th}(x)\} = R_{Th}(\theta) = E\{\delta_{Th}(X) - \theta\}^2 \tag{5.48}$$

Note that $X = N(\theta, 1)$.

5.7.5 S-Median Threshold

In the theory of nonparametric regression, the recovery of the unknown function $f(x)$ from the noisy observation on equi-spaced location x_N is measured using MSE. The function after the addition of noise can be represented as

$$y = f(x_i) + \varepsilon_i, i = 1,2,\ldots,n \tag{5.49}$$

where ε is White Gaussian noise with i.i.d. $N(0,\sigma^2)$ and $f(x_i)$ samples of deterministic function f. The MSE of the function (henceforth called Risk) is determined as

$$MSE(\hat{f}, f) = \frac{1}{n} \sum_{i=1}^{n} E\left\{ f(\hat{x}_i) - f(x_i) \right\}^2 \tag{5.50}$$

The primary aim of denoising model is to keep the risk as low as possible, that is, the recovered signal would be same as the original signal. A higher value for risk would invariably mean more deviation of the recovered signal from the original signal. This is not desirable. Keeping this into consideration, a level dependent threshold has been designed, which will harness the spatial adaptivity of the WT and at the same time preserve the noise free reconstruction property [60]. The proposed threshold minimizes the value of MSE and outperforms the universal threshold in the process. As the universal threshold and other thresholds have their effect on the noisy signal globally, there are deprived of the spatial property, which varies for sub bands. The universal threshold being globally adaptive is denied the flexibility of being local to subbands. As a result it over smoothens the signal. On the other hand, S-median is locally adaptive and hence flexible to the subband levels. The presence of a tuning factor, which tunes the threshold to each and every subband level, helps in achieving effective denoising of signal [60]. This enables to attain lower risk than the universal threshold. The subband level dependent median threshold (S-median) inherits optimality in MSE as well as spatial adaptivity along with subband level adaptivity. S-median threshold is defined as

$$Th_{l,k} = \frac{\sigma_k \sqrt{2\log(n)}}{(S_{l,k} + b)}, k = 1,2,\ldots,l \tag{5.51}$$

where $S_{l,k}$ is sub band level dependent parameter, denied as

$$S_{l,k} = 2^{(L-K/L)} \tag{5.52}$$

where L is deepest decomposition level to which signal is decomposed and K is level at which thresholding is done (for example at level 3, K = 3). Apart from spatial adaptation and optimality, S-median has tuning factor b, which tunes the threshold to obtain effective noise-free reconstruction unlike universal threshold, which over smoothens by killing significant coefficients. σ is noise variance of the noisy signal. If noise variance of the noisy signal is not known, one has to estimate via the median absolute deviation (MAD) estimator proposed by the Donoho on all thelevels, that is

$$\sigma_k = \frac{median|x|}{0.6745}, k = 1,2,\ldots,l \tag{5.53}$$

5.7.6 Modified S-Median Threshold

We proposed a level dependent adaptation factor $\left(\frac{L}{k}\right)$ in equation 5.51. So that DBWT can perform better. In addition with the adaptation factor , optimum value of the tuning factor b can make the system more sophisticated. Finally our proposed modified S-median thresholding equation is :

$$Th_{l,k} = \left(\frac{L}{k}\right)\frac{\sigma_k\sqrt{2\log(n)}}{(S_{l,k}+b)}, k = 1,2,\ldots,l \tag{5.54}$$

The optimum value of b is achieved where the highest SNR improvement exist. For different types of noise, the characteristic curve of b is shown in Fig 5.14 and Fig 5.15.

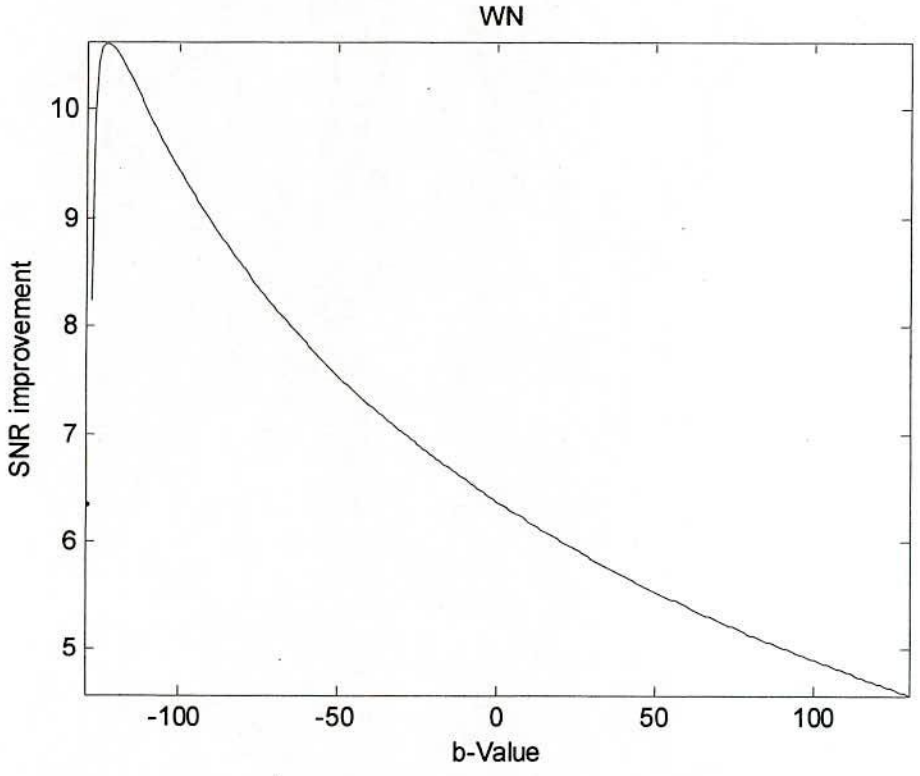

(a) Characteristic curve of b for White noise

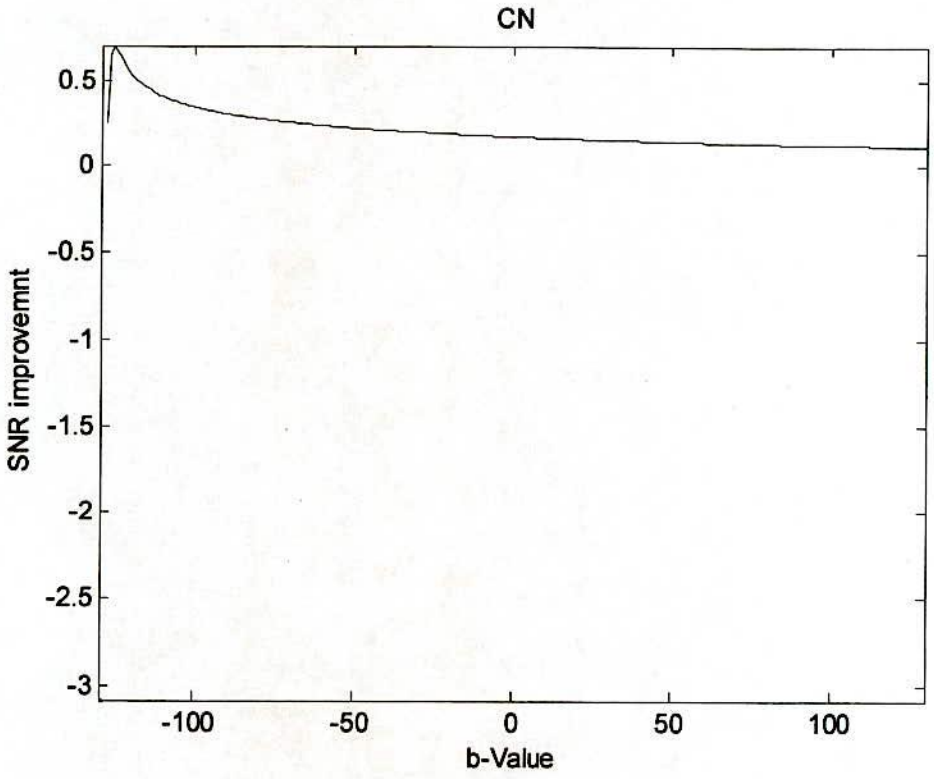

(b) Characteristic curve of b for colored noise

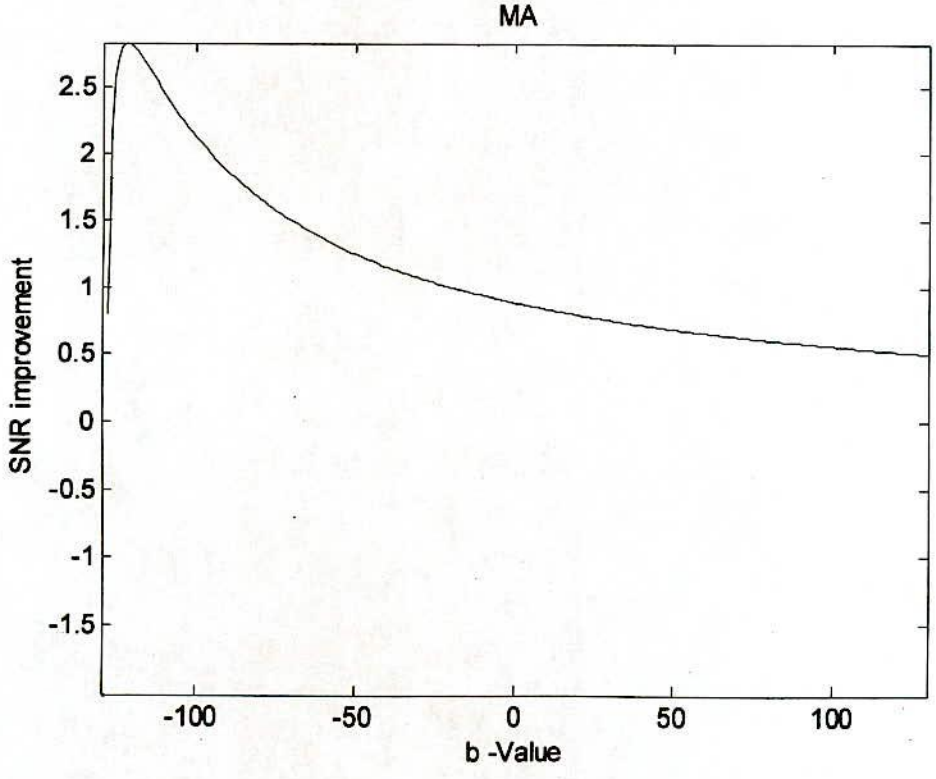

(c) Characteristic curve of b for Muscle artifact noise

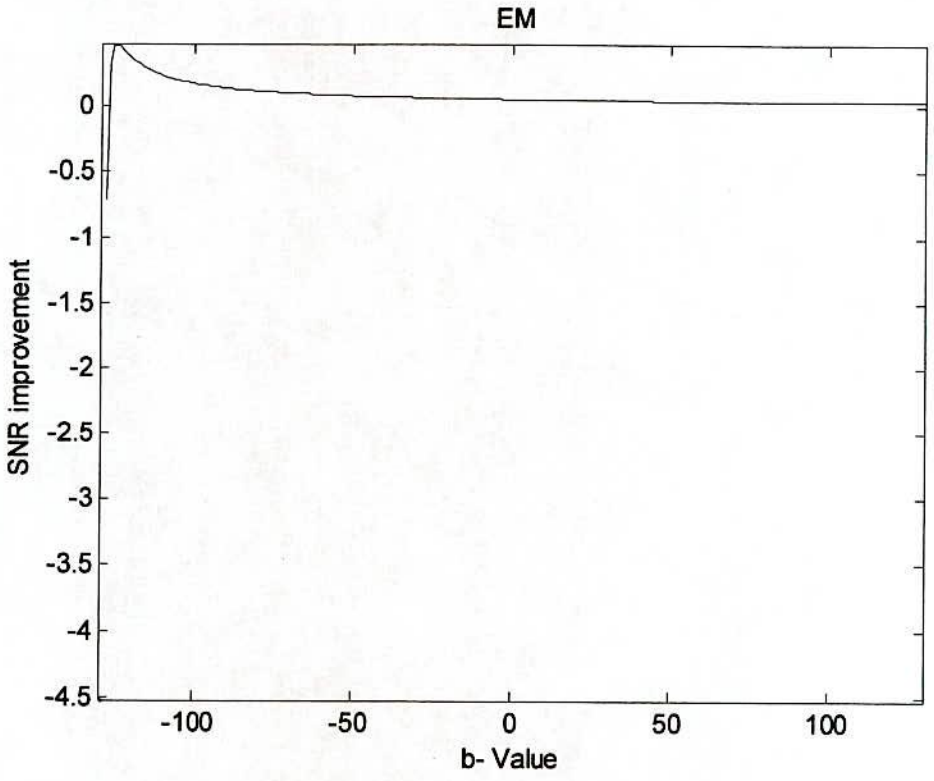

(d) Characteristic curve of b for electrode movement noise

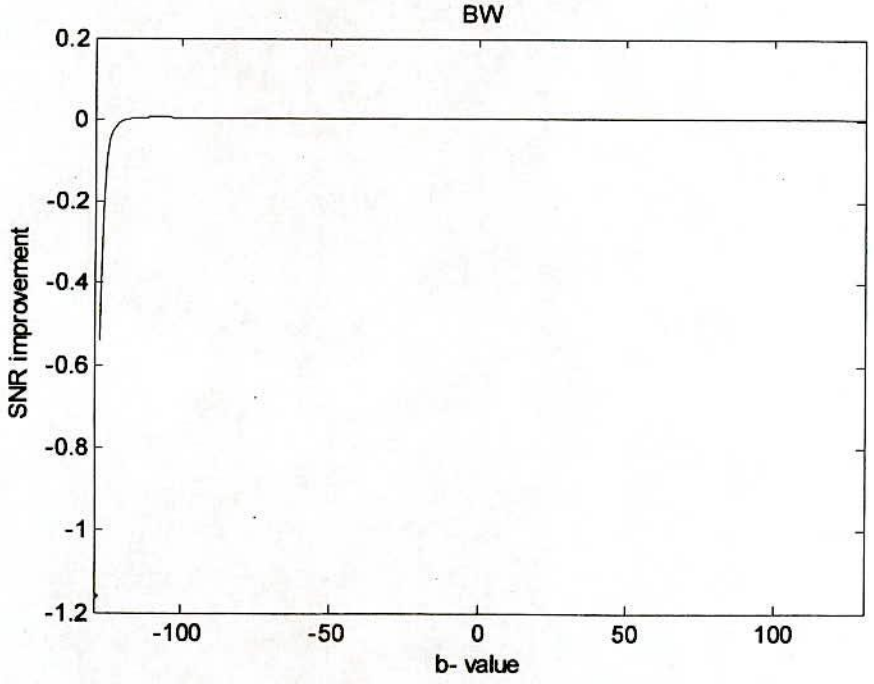

(e) Characteristic curve of b for Baseline Wander

Figure 5.14 (a-e): Characteristic curve of b for different noise.

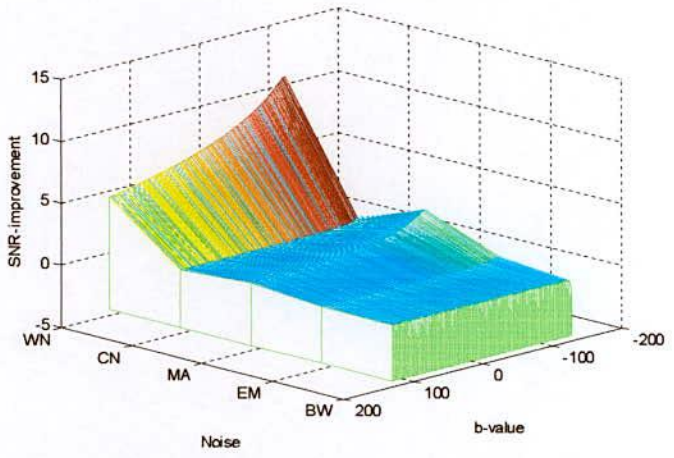

Figure 5.15 : The total reflection of b against different types of noise and SNR improvement.

5.8 Data Acquisition

For the MIT-BM Arrhythmia Database, [61] attempted to obtain a representative sample of the variety of recordings which were observed in clinical practice. This database consists of 48 annotated records, obtained from 47 subjects studied by the Arrhythmia Laboratory of Beth Israel Hospital in Boston between 1975 and 1979. About 60% of the records were obtained from inpatients. The database contains 23 records (the '100 series') chosen at random from a set of over 4000 24-hour Holter tapes, and 25 records (the '200 series') selected from the same set to include a variety of rare but clinically important phenomena which would not be well-represented by a small random sample. Several records in the 200 series were chosen specifically because features of the rhythm, QRS morphology, or signal quality may be expected to present significant difficulty to arrhythmia detectors. These records have gained considerable notoriety among users of the database. In the MIT-BIH Arrhythmia Database, there is considerable variation in signal quality, with significant portions of unreadable data in at least one lead. Among the above records we chose 20 records for our research purpose.

Real data are collected by BIOPAC data acquisition system from the Biomedical signal processing laboratory , Khulna University of Engineering and Technology . More details about the data acquisition has been in discussed in section 4.2.

5.9 Summarization and Evaluation of the proposed Transform

5.9.1 Summarization

Data were collected as described in section 4.2 . The ECG denoising using WT can be described as the following algorithm.

5.9.1.1 Signal denoising algorithm

a) Decompose

Transform the signal into wavelet domain selecting the level of decomposition using commonly supported orthogonal wavelet bases (Daubechies, Coiflets and symmlets).

b) Threshold detail coefficients

For each level from 1 to N, select a threshold method (like SURE, Heuristic, Minimax, universal, s-median and our modified s-median). Then a soft and hard thresholding is applied to the detail coefficients and rescaling is done using a single estimation of level noise based on first level coefficients.

c) Reconstruct

Compute wavelet reconstruction based on the original approximation coefficients of level N and the modified detail coefficients of levels from 1 to N.

The using DBWT (shown in Fig 5.16) and adaptive thresholding process the signal was denoised and performance were evaluated by MSE, NMSE, RMSE, NRMSE, PRD like section 3.4.5 and SNR improvement was calculated using following equation [62] :

$$imp_{dB} = 10\log\left(\frac{\sum_{n=0}^{N-1}[x_n(n)-x(n)]^2}{\sum_{n=0}^{N-1}[x_R(n)-x(n)]^2}\right) \tag{5.54}$$

Where $x_n(n)$ is the noisy ECG data.

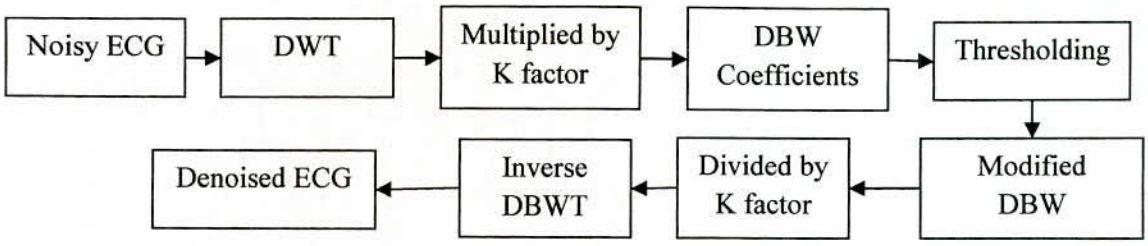

Figure 5.16 : Block Diagram of the proposed DBWT technique.

5.9.2 Evaluation of the proposed Transform

5.9.2.1 Performance Evaluation in Time Domain

Wavelet transform represents a given function f in a very efficient way by using a set of basic functions. In this research, these basic functions are referred as wavelet families. Some of the most famous wavelet families are Daubechies, Coiflet and Symlet are like the shape of ECG signal. Here, we show them by dbN, coifN and symN, respectively, where N indicates the order. The DWT were performed by these wavelet family and theses DWT coefficients are used for our proposed DBWT.

To find the suitable wavelet function (db3,db4,db5,coif3, coif4, coif5, sym 3, sym4, sym5) from the above wavelet family, we used different types of error measurement techniques. The performance was analyzed on our recorded ECG data with input SNR 5dB and decomposition level was 7. From Table 5.2, it was observed that most of the wavelet functions shows SNR improvement around 12 dB except coif4 which was 13.0192185 dB. So from this data it was clear that coif4 was the best suited wavelet function for our proposed DBWT.

Table 5.2: Finding of best wavelet function for DBWT

WT function	SNR imp(dB)	MSE	NMSE	RMSE	NRMSE	PRD(%)
db3	12.4245477	0.00064228	0.01808536	0.025343215	0.00032708	0.032708016
db4	12.8273353	0.00058539	0.01648346	0.024194816	0.000271704	0.027170441

db5	12.6829876	0.00060517	0.01704053	0.024600261	0.00029038	0.029037969
coif3	12.6218382	0.00061375	0.01728216	0.02477406	0.000298673	0.029867311
coif4	13.0192185	0.00056009	0.01577103	0.023666181	0.000248725	0.024872536
coif5	12.2389963	0.00067031	0.0188748	0.025890431	0.000356258	0.03562579
sym3	12.4095103	0.00064451	0.01814809	0.025387128	0.000329353	0.032935305
sym4	12.579667	0.00061974	0.01745079	0.024894634	0.00030453	0.030453019
sym5	12.8530417	0.00058193	0.01638618	0.024123316	0.000268507	0.026850688

When we performed wavelet, the number of level is also an important decisive factor. To solve this concern different level were calculated to find an optimum level. From table 5.3, it was clear that after level 7, the performance was almost saturated and the best result was found in level 8.

Table 5.3: Different performance parameter for various level of coiflet wavelet transform for the proposed DBWT.

No. of level	SNR imp(dB)	MSE	NMSE	RMSE	NRMSE	PRD(%)
12	13.05858851	0.000555	0.015629	0.023559	0.000244	0.024426
11	13.03240673	0.000558	0.015723	0.02363	0.000247	0.024722
10	13.01713124	0.00056	0.015779	0.023672	0.000249	0.024896
9	13.03340335	0.000558	0.01572	0.023628	0.000247	0.024711
8	13.04864645	0.000556	0.015665	0.023586	0.000245	0.024538
7	13.01921847	0.00056	0.015771	0.023666	0.000249	0.024873
6	12.91837203	0.000573	0.016142	0.023943	0.000261	0.026055
5	12.52024458	0.000628	0.017691	0.025066	0.000313	0.031298
4	11.78618176	0.000744	0.020949	0.027276	0.000439	0.043886
3	9.340271831	0.001307	0.036792	0.036147	0.001354	0.135366
2	6.277643606	0.002645	0.074476	0.051429	0.005547	0.55467
1	2.988445672	0.005641	0.158832	0.075105	0.025228	2.522752

In order to test the S-median threshold [60] from a different perspective, SNR values were obtained by the simulation of the noisy signals. The comparison was made among SURE, Heuristic ,Universal, Minimax, S-median and finally our proposed techniques. The results showed that our modified S-median performed good with wide range of noises as shown

in table 5.4. This is due to its spatial adaptivity and subband dependency. In the case of white noise, the SNR values of universal threshold were low due to its over smoothening effect. But SURE method worked like our proposed method. Heuristic and Minimax showed moderate results. In the case of color noise our method was the best and Universal thresholding took second place. And other noises like real muscle artifact noise, real electrode movements noise and composite noise our method was the best.

Table 5. 4: Performance of different thresholding techniques in various noises for MIT-BIH Arrhythmia database of record no 101 with input SNR 5 dB.

Thresholding method	SNR improvement (dB)				
	White noise	Color noise β=1	Real muscle Artifact noise	Real electrode movements noise	Composite noise
SURE	9.450735621	0.754034254	0.007468091	0.004137153	0.004964368
Heuristic	8.601119038	0.756901556	0.007468091	0.003748027	0.004964368
Universal	3.849764406	1.951622539	0.169844849	0.034671279	0.101521614
Minimax	6.180948816	1.854957389	0.116736434	0.026509489	0.07238152
S-median	1.456083658	0.496454865	0.109088544	0.02736789	0.050137164
Proposed	9.066188459	2.047015606	0.354128856	0.21632556	0.138465323

In order to make a comparison among conventional wavelet based ECG denoising schemes WT, Multiadaptive Bionic Wavelet Transform (MABWT) [63] and our proposed DBWT were tested on database. The result of SNR improvement for the input SNR of 5dB are listed in Table 5.5.

According to these result, our proposed hard thresholding was little bit smaller (0.03 dB) than MABWT hard thresholding which was negligible. However, our proposed DBWT soft thresholding performance is always better (average 9.508164 dB), than the corresponding techniques. Because [63] used T-function derived from the active auditory model of the cochlea. But in our case, we used T-function derived from heart-arterial interaction model . As ECG is the electrical activity of heart, so our system is more appropriate for this particular problem.

Table 5.5: WT, MABWT [63] and Proposed DBWT denoising performance on the MIT-BIH arrhythmia database.

MIT-BIH Record No.	SNR improvement (dB)					
	WT (hard)	WT (soft)	MABWT (hard)	MABWT (soft)	Proposed DBWT (hard)	Proposed DBWT (soft)
100	5.1	6.5	6.4	7.8	6.4236	9.4670
101	4.2	5.5	5.3	6.9	7.0352	9.335
103	5.0	6.1	5.8	7.7	5.7398	8.9308
105	5.1	6.0	5.8	8.1	5.8051	9.6645
112	5.2	6.4	6.1	8.2	6.7078	11.3956
113	5.0	6.2	5.9	7.9	5.9202	9.2529
115	5.1	6.6	6.3	7.8	6.0656	9.9985
116	5.0	6.5	6.4	8.0	5.0921	9.5638
117	4.8	6.0	5.8	7.9	5.2178	11.4554
119	4.7	5.8	5.6	7.6	4.5820	10.1557
122	4.4	5.6	5.2	6.9	4.6599	10.2348
123	5.1	6.5	6.4	7.8	4.5002	10.5943
200	4.2	5.4	5.3	6.9	6.0859	9.1397
201	5.0	5.4	5.5	7.5	5.8562	9.2680
202	4.9	5.8	5.7	7.8	6.3814	10.1448
205	5.0	5.4	5.5	7.4	5.6521	9.2076
209	5.2	6.0	5.9	8.1	5.4962	8.2447
210	4.3	5.4	5.3	6.9	6.3475	9.5318
212	4.0	5.0	4.8	6.7	5.6953	8.5329
213	5.2	6.6	6.4	8.2	5.5305	8.5548
219	5.2	6.5	6.3	8.0	5.7963	10.0070
220	5.1	6.5	6.4	8.1	5.7718	9.5384
221	4.9	6.0	5.9	7.9	6.0551	9.3020
230	5.0	5.9	5.6	7.9	5.7265	8.8722
233	4.8	5.8	5.5	7.8	6.0672	7.3119
Average	4.86	5.98	5.80	7.67	5.768452	9.508164

We also made another comparison with TQWT. Q-factor in TQWT can be change to 2,3,4 etc. which demonstrated that lower Q is not suitable for oscillatory signal like ECG. In contrast, our proposed model tuning is achieved by the signal's instantaneous value and it's first difference. To express this phenomena we compare TQWT with various Q value of 2,3,4,5 with our proposed variable Q wavelet like DBWT in table 5.6. To run the TQWT program we used TQWT software which is available and free of cost in the MATLAB environment [42]. As can be observed from the table 6, Q=2 of TQWT perform best among different Q. But our system is far much better than the TQWT of Q=2 with a SNR improvement of 9.411715849 dB.

Table 5.6: Denoising performance comparision between TQWT and Proposed DBWT on the MIT-BIH arrhythmia database.

MIT-BIH Record No.	SNR improvement for input SNR 7dB					
	Tunable Q Wavelet Transform				Proposed	
	Q=2	Q=3	Q=4	Q=5	Hard	Soft
100	5.545270342	3.952637082	2.386310636	1.348847271	5.413129028	8.958326806
101	5.554463579	4.050350608	2.478236207	1.435116116	5.306100576	9.00766596
103	5.603835981	4.144304568	2.716462592	1.87086842	4.835908202	8.479137735
105	6.08639478	4.329981108	3.05706826	1.951020237	5.998428297	9.38433215
106	5.552894361	4.246907913	2.980817092	2.183583309	4.594580802	8.191453107
107	2.978130748	2.799168	2.386911552	2.137531386	5.670935428	9.374657705
108	6.028420386	4.281459717	2.591005752	1.485685461	6.457281989	10.23911025
109	4.572837733	3.923694999	2.90823931	2.215287709	5.818305634	9.818249903
111	5.087043841	2.870470843	1.148959602	0.020280995	5.2933516	8.550925499
112	2.931328044	2.667410053	2.19704942	1.838214175	6.278200689	10.79492196
113	5.117555	4.249956251	3.091593194	2.383806289	5.483397993	8.42550176
115	3.963627476	3.400923982	2.633107799	2.089203629	6.070400401	9.628817456
116	2.347879956	2.19606694	1.87513444	1.63803271	4.226886998	8.997243191
117	3.251555754	2.927055753	2.381381137	2.001973532	6.628341431	11.31534583
119	2.533591787	2.358181846	1.977967578	1.696028126	4.573396167	9.757129429
122	2.81029976	2.600125818	2.151332937	1.813920638	6.263098283	10.27372836
223	4.350076619	3.871691956	3.299157622	2.746852401	5.707212871	8.802622341
Average	4.371482715	3.462963967	2.485925596	1.815073671	5.565820964	9.411715849

5.9.2.2 Performance Evaluation in Frequency Domain

The proposed method is evaluated not only in time domain but also frequency domain using DFT and MSC. In Fig. 5.17, original and reconstructed ECG signal are almost identical all over the frequency domain. An another important criteria shows in frequency domain is most of the information of the ECG signal lies between 0Hz to 50Hz.

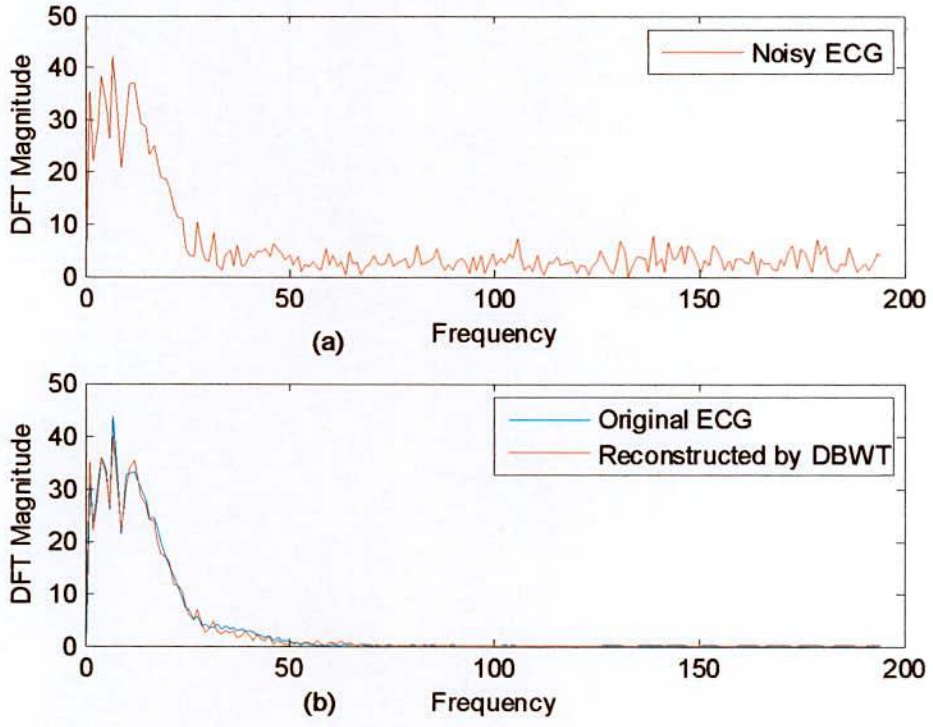

Figure 5.17 : Frequency domain analysis using DFT. (a) Noisy ECG with White noise of SNR 5 dB. (b) Comparison between original and reconstructed ECG by DBWT. The Original ECG was collected using BIOPAC system.

MSC is used to examine the relation between two signals or data sets with values between 0 to 1. 1 indicates identical two signals are identical in frequency domain whereas 0 indicates the opposite. Here this concept was used to illustrate the frequency domain performance of DBWT and TQWT. In Fig. 5.18 , it can be observed that the MSC is almost unity over dominated frequency region whereas this statement was deviated. They had a downward spike in low frequencies which is marked as shaded box in the figure.

This means that TQWT eliminate some of low frequency component of ECG signal which carries important information.

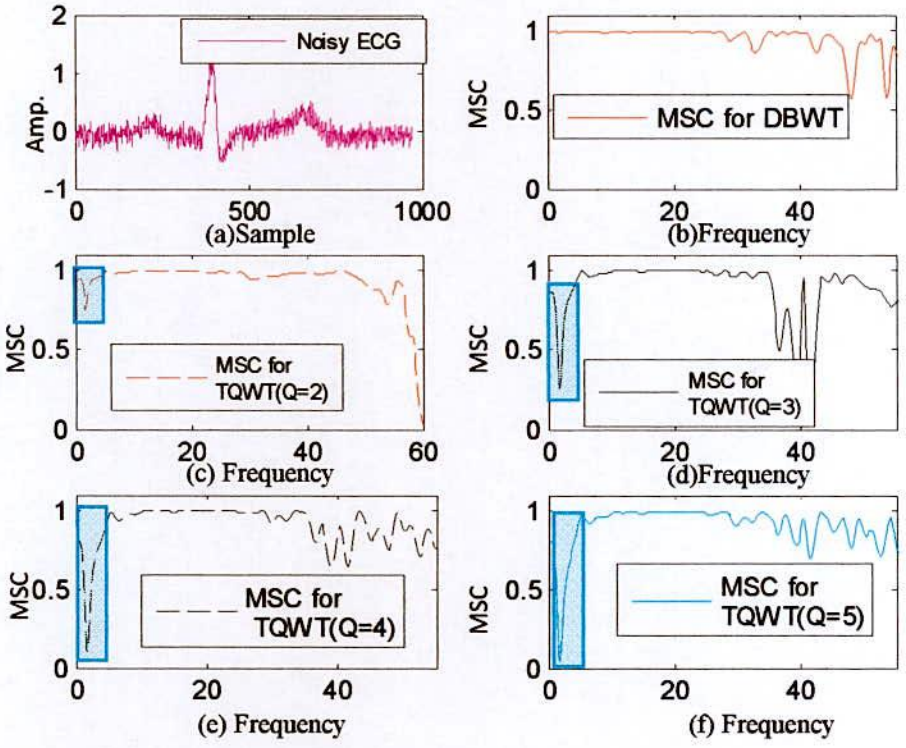

Figure 5.18: (a) Noisy ECG signal, (b-f)Magnitude Squared Coherence (MSC) of different WT.

CHAPTER VI

CONCLUSION AND FUTURE SCOPE

6.1 Conclusion

Cardiac conditions is determined by ECG. But different types of noise can lead misdiagnosis. So, denoising ECG signal is an active area of research worldwide. The method developed here are based on cardiac model so it is more suitable for denoising the ECG. In this research, model based ECG denoising techniques is developed using DBWT and application of this transform is also illustrated to classify the Cardiac conditions using SVM.

The proposed model is capable of replicating many important features of the human ECG wave. A number of features and applications of the model are: (i) Instead of using too many parameters like other model do, the proposed one can generate ECG and in capable of simulating various kinds of practical phenomena such as brachycardia, tachycardia and so on using few parameters. (ii)It does not need three dimensional state spaces which are difficult for realization and simulation. (iii)Noisy ECG signal can be modeled simply by adding a noise parameter to the model. (iv) In frequency domain the real and modeled ECG showed almost same properties. (v)A realistic ECG database can be created by fitting the model with individual subject's ECG. This can be used for further analysis and also for education purposes. (vi)By saving the coefficient of the model alone ECG data compression can be possible. However, the lower value of error parameters like MSE 0.0023 and 0.0291 for recorded and MIT-BIH database respectively indicates the effectiveness of this simplified model and the proposed model enables us to investigate wave morphology variation. It can be further improved for better fitting, model-based denoising, compression and support vector machine classification etc. Finally, it is hoped that this simple model will provide an efficient tool for testing and processing of the ECG signals with different level of noise and/or motion artifact.

In this research, a novel DBWT based adaptive thresholding techniques were presented for different types of realistic noise. The T-function stemming from active biological model of heart-arterial interaction model performs well when being applied to cardiac signal processing. With the improvement of the heart-arteial model, a better performance of DBWT was achieved. Generally, for different applications, different T-functions should be used. One possible choice of T-function can be made according to the cardiac signal's instantaneous value and its first difference value. For example, in case of ECG signal, the T-function based on the heart-arteial model is a natural choice. The active mechanism of the cardiac model compared to the traditional WT, special properties of DBWT can be summarized as follows:

- A new parameter T, controlled by the signal's instantaneous amplitude and its first-order differential, is introduced with the WT. With this additional parameter, the adaptive adjustment of resolution has been implemented.
- The constant Q of traditional WT and tunable in TQWT is replaced with variable Q.
- DBWT is a nonlinear transform which has high sensitivity and frequency selectivity.
- The inverse transform of DBWT exists, which makes the utilization of BWT possible in signal coding and decoding of signals.

The effectiveness of the proposed method in ECG denoising was shown experimentally and also through simulations from standard database like MIT-BIH. Compared with other thresholding methods such as SURE, heuristic, minimax, universal and S-median our proposed thresholding method gives SNR improvement of 9.066188459 dB and 2.047015606 dB respectively in the presence of Gaussian and colored noise which is better than mentioned techniques. The proposed transform gives outstanding performance with average SNR improvement of 9.508164 dB whereas in WT, MABWT and TQWT the values were 5.98dB, 7.67dB and 4.371482715 dB (Q=2) respectively. Moderate result was achieved in the presence of baseline wander, motion artifact, and electrode movement noise.

6.2 Future Scope

A frequency domain pre-processing step before applying the thresholding, different wavelet filter bank and more efficient thresholding function may achieve a better result which is taken under consideration. In future, the model can be used for wide range of applications such as compression of signal, automatic diagnosis system and so on. The proposed techniques can be applied not only in ECG but also other bio-signal like EMG, EOG etc.

REFERENCES

[1] G. D. Clifford, F. Azuaje, P. E. McSharry, "Advanced Methods and Tools for ECG Data Analysis", Artech House, Inc, 2006.

[2] C. P. Behrenbruch, "SNR improvement, filtering and spectral equalization in cochlear implants using wavelet techniques," Proc. 2nd Int.Conf. Bioelectromagnetism, pp. 61–62, 1998.

[3] K. Nie, N. Lan, and S. Gao, "Implementation of CIS speech processing strategy for cohlear implants by using wavelet transform," in Proc. ICSP'98, pp. 1395–1398.

[4] J. Yao and Y. T. Zhang, "Bionic wavelet transform: a new time-frequency method based on an auditory model," IEEE Transactions on Biomedical Engineering, vol. 48, no. 8, pp. 856–863,2001.

[5] G.M. Friesen et. al, "A comparison of the noise sensitivity of nine QRS detection algorithms", IEEE Transactions on Biomedical Engineering , Vol. 37, no. 1, 85–98,(1990).

[6] J. G. Webster, "Medical Instrumentation-Application and Design", Boston: Houghton Mifflin, 2nd Ed. 1978.

[7] www.physionet.org/.

[8] Biopac Student Lab 3.7, BIOPAC System, Inc., 2008.

[9] I. S. N. Murthy, Mandayam R. Rangaraj, K. Jayaram Udupa, A. K. Goyal, "Homomorphic Analysis and Modeling of ECG Signals," IEEE Trans Biomed Eng., vol. BME-26 Issue:6 pp. 330 - 344,June 1979.

[10] I.S.N. Murthy, G.S.S.D. Prasad, "Analysis of ECG from pole-zero models," IEEE Trans Biomed Eng., vol: 39, issue:7 pp. 741 - 751,July 1992.

[11] L. Sörnmo, PO. Börjesson, ME. Nygårds, O. Pahlm, "A method for evaluation of QRS shape features using a mathematical model for the ECG", IEEE Trans Biomed Eng. vol. 28, issue 10, pp.713-7,Oct. 1981.

[12] W. Philips, and G. De Jonghe. "Data compression of ECG's by high-degree polynomial approximation ". IEEE Trans. Biomed. Eng., vol.39,issue 4, pp. 330-337, 1992.

[13] B. Madhukar, and I. S. N. Murthy. "ECG Data Compression by Modeling". Comput. Biomed. Res.26:310-317, 1993.

[14] S. Suppappola, Y. Sun, SA. Chiaramida, "Gaussian pulse decomposition: An intuitive model of electrocardiogram waveforms," Annals of Biomedical Engineering. vol. 25, no. 2 pp. 252-260 , Mar-Apr, 1997.

[15] G.D. Clifford, A. Shoeb, P. E. McSharry, BA. Janz , "Model based filtering, compression and classification of the ECG," International Journal of Bioelectromagnetism, vol. 7, no 1 pp.158-161, 2005.

[16] G.D. Clifford, "A Novel Framework for Signal Representation and Source Separation: Applications to Filtering and Segmentation of Biosignals," Journal of Biological Systems. vol. 14, no 2, pp.169-183, Jun 2006.

[17] P.E. McSharry , G.D. Clifford , L. Tarassenko, L. Smith , "A Dynamical Model For Generating Synthetic Electrocardiogram Signals," IEEE Trans Biomed Eng., vol. 50, issue 3, pp. 289–294, Mar 2003.

[18] G.D. Clifford, M. Villarroel, "Model-Based Determination of QT Intervals," Computers in Cardiology,vol.33(k53) pp.357-360, Sep 2006; IEEE Computer Society Press..

[19] S. Parvaneh, M. Pashna, "Electrocardiogram Synthesis Using a Gaussian Combination Model (GCM) ,"Computers in Cardiology vol. 34, pp.621−624, 2007.

[20] J. Richardson, L.J. Haywood, V.K. Murthy and G. Harvey "A mathematical model for ECG wave forms and power spectra", Mathematical Biosciences, vol. 12, issues 3-4, pp. 321-328, Dec 1971.

[21] M.A.Awal, S.S. Mostafa,and M. Ahmad, "Performance Analysis of Savitzky-Golay Smoothing Filter Using ECG Signal", International Journal of Computer and Information Technology, vol. 01, no. 02, January 2011.

[22] R.Vullings, B.D.Vries, and J.W.M. Bergmans, "An Adaptive Kalman Filter for ECG Signal Enhancement", IEEE Transactions on Biomedical Engineering, Vol. 58, No. 4,pp 1094-1103, April 2011.

[23] S.Butterworth, "On the theory of filter amplifiers," Exp. Wireless Eng., vol. 7, pp. 536–541, Oct. 1930.

[24] W.H. Press, S.A. Teukolsky, W. T. Vetterling, B. P. Flannery, Numerical recipes in C++, 2nd ed, Cambridge University Press 2002.

[25] Brigham, E.O. The Fast Fourier Transform and Its Applications, Englewood,NJ: Preintice-Hall, 1988.

[26] Welch, P. D. ,"The use of fast Fourier transform for the estimation of power spectra: a method based on time averaging over short, modified periodograms," IEEE Trans. Audio Electroacoustic, vol. AU-15, pp. 70–73, June 1967.

[27] M.S.Manikandan, S.Dandapat,"Wavelet energy based diagnostic distortion measure for ECG", Biomedical Signal Procesing and Control, vol 2, issue 2, pp 80-96, Apr 2007.

[28] R. M. Rangayyan, Biomedical Signal Analysis: A Case-Study Approach, Series on

Biomedical Engineering, New york: Wiley-IEEE Press, 2002.

[29] K. R. Borisagar and G.R. Kulkarni "Simulation and Comparative Analysis of LMS and RLS Algorithms Using Real Time Speech Input Signal", Global Journal of Researches in Engineering, Vol.10 Issue 5 October 2010.

[30] S.M. Kuo and D.R.Morgan, "Active Noise Control: a tutorial review", Proceedings of the IEEE, Vol. 87, No. 6, June 1999.

[31] R. Cohen and A. Ryan, Wavelets and Multiscale Signal Processing, London, U.K.:Chapman and Hall, 1995.

[32] W. Williams, "Recent Advances in Time-Frequency Representations: Some Theoretical Foundation," in M. Akay, (ed.), Time Frequency and Wavelets in Biomedical Signal Processing, Chapter 1, New York: Wiley-IEEE Press, 1997.

[33] M. Misiti, Y. Misiti, G. Oppenheim, J.M. Poggi, Wavelet Toolbox User's Guide, The MathWorks, Inc. 1996 – 1997.

[34] F. Chen, and Y.T.Zhang "A new implementation of discrete bionic wavelet transform: Adaptive tiling", Digital signal processing, vol. 16 issue 3 pp.233-24, 2006.

[35] X. Yuan, "Auditory model-based bionic wavelet transform for speech enhancement," M.S. thesis, Speech and Signal Processing Laboratory, Marquette University, Milwaukee, Wis, USA,2003.

[36] S. Mallat, A Wavelet Tour of Signal Processing, 3rd ed. Academic Press, dec. 2008.

[37] C. K. Chui, Wavelets: A Tutorial in Theory and Applications , Vol. 2, Academic Press (January 31, 1992).

[38] I. Daubechies, Ten Lectures on Wavelets, SIAM: Society for Industrial and Applied Mathematics; 1st ed. , June 1, 1992.

[39] P.J.V. Fleet, Discrete wavelet transformation, John Wiley & Sons Inc. Publication, 2008.

[40] I. W. Selesnick, "Wavelet Transform with Tunable Q-Factor",IEEE Trans. on Signal Processing. Vol. 59 issue 8 ,pp 3560-3575, August 2011. .

[41] I. Bayram and I. W. Selesnick, " Frequency-domain design of overcomplete rational-dilation wavelet transforms", IEEE Trans. on Signal Processing, Vol. 57 no 8,pp: 2957-2972, August 2009.

[42] http://eeweb.poly.edu/iselesni/TQWT/index.html.

[43] X. Y. Zhang and Y.T. Zhang, "A Model-based Study of Relationship between Timing of Second Heart Sound and Systolic Blood Pressure", IEEE -EMBS Annual International

Conference, New York City, USA, Aug 30-Sept 3, 2006.

[44] J.K-J Li, Dynamics Of The Vascular System, World Scientific Publishing Co. Re. Ltd.2004.

[45] M. Karamanoglu, D. E. Gallagher, A. P. Avolio, and M. F. O'Rourke "Pressure wave propagation in a multibranched model of the human upper limb." Am. J. Physiol. 269 (Heart Circ. Physiol. 38): H1363–H1369, 1995.

[46] P.Segers et.al. "Individualizing the aorto-radial pressure transfer function: feasibility of a model-based approach" Am J Physiol Heart Circ Physiol. Vol.279: H542–H549, 2000.

[47] B.E. Westerhof et. al. "Arterial pressure transfer characteristics: effects of travel time". Am. J Physiology Heart Circ Physiology Vol.292: H800–H807, 2007.

[48] M. T.Stephanie, J. Melbin, A. Noordergraaf, "Reduced Models of Arterial Systems" , IEEE Transactions on Biomedical Engineering, Vol. Bme-32, No. 2, February 1985.

[49] M. Sugimachi, T. Kawada, T. Shishido1, N. Matsumoto,J. Alexander, Jr., K. Sunagawa, "Estimation of Arterial Mechanical Properties from Aortic and Tonometric Arterial Pressure Waveforms" , Methods of Information in Medicine, Vol.36: 250-3, 1997.

[50] M. Sugimachi, T.Shishido, K. Miyatake, K.Sunagawa, "A new model based method of reconstructing central aortic pressure from peripheral arterial pressure", Jpn J Physiol Vol.51: 217–222, 2001.

[51] J.J.Wang,J.A.Flewitt,N.G. Shrive,K.H Parker,J.V Tyberg,"Systemic venous circulation. Waves propagating on a windkessel:relation of arterial and venous windkessels to systemic vascular resistance." Am J Physiology Heart Circ. Physiology290:H154–H162, 2006.

[52] J. Yao and Y. T. Zhang, "From otoacoustic emission modeling to bionic wavelet transform," in Proceedings of the 22nd Annual International Conference of the IEEE Engineering in Medicine and Biology Society, vol. 1, pp. 314–316, Chicago, Ill, USA, July2000.

[53] B.E. Westerhof et. al. "Individualization of transfer function in estimation of central aortic pressure from the peripheral pulse is not required in patients at rest." J Appl Physiol 105: 1858–1863, 2008..

[54] M. T. Johnson, X. Yuan, Y. Ren, "Speech signal enhancement through adaptive wavelet thresholding", Speech Communication, Vol. 49 issue 2, pp 123-133, 2007.

[55] M. Jansen, "Noise reduction by wavelet thresholding", New York: Springer-Verlag; 2001.

[56] D.L. Donoho, "Denoising by soft thresholding", IEEE Trans Inform Theory Vol.41no. 3 pp:613–27. 1995.

[57] D.L. Donoho, I.M. Johnstone, "Ideal spatial adaptation via wavelet shrinkage. Biometrika, vol.81issue 3 pp:425–55,1995.

[58] S.G. Chang, B.Yu, M. Vetterli, "Adaptive wavelet thresholding for image denoising and compression", IEEE Trans Image Process vol. 9 pp:1532–46, 2000.

[59] Q. Fu, E.A. Wan, "Perceptual wavelet adaptive denoising of speech" In: EUROSPEECH. pp. 578–80,2003.

[60] S. Poornachandra, "Wavelet-based denoising using subband dependent threshold for ECG signals", Digital Signal Processing, vol. 18 pp:49–55,2008.

[61] G.B. Moody and R.G. Mark, "The MIT-BIH Arrhythmia Database on CD-ROM and software for use with it", Computers in Cardiology,pp: 185-188,1990.

[62] O.Sayadi, M.B. Shamsollahi, G.D. Clifford, "Synthetic ECG Generation and Bayesian Filtering Using a Gaussian Wave-based Dynamical Model", Journal of Physiological Measurement, 2010..

[63] O. Sayadi, and M. B. Shamsollahi, "Multiadaptive BionicWavelet Transform: Application to ECG Denoising and Baseline Wandering Reduction", EURASIP Journal on Advances in Signal Processing, vol. 2007, 2007.

[64] J. R. Womersley, "The mathematical analysis of the arterial circulation in a state of oscillatory motion", Wright Air Development Centre, Technical Report, WADC-TR56-614, 1957.

[65] D. A. McDonald, 'Blood flow in Arteries', Arnold, London, 2nd ed. , 1974.

[66] B. Duan, M. Zamir, "Pressure peaking in pulsatile flow through arterial tree structures", Annals of biomedical Engineering, Vol. 23, pp. 794-803, 1995.

[67] A. P. Avolio , "Multi-branched model of the human arterial system", Med. & Biol. Eng. & Comput., vol. 18, pp: 709 718,1980.

[68] S. Shin, Y. Park, H. Rhim, W. Yoo, D. Park, "Multibody Dynamics In Arterial System", Proceedings of ACMD, 2004.

[69] D. H. Bergel, "The dynamic elastic properties of the arterial wall", J. Physiol. Vol. 156, issue 3,1961.

[70] M. G. Taylor, "The experimental determination of the propagation of fluid oscillations in a tube with a viscoelastic wall; together with an analysis of the characteristies required in an electrical analogue".

[71] N. Westerhof and A. Noordergraf, "Arterial viscoelasticity: a generalised model", J. Biomech. vol. 3, 1970.

[72] M. G. Taylor, "The input impedance of an assembly of randomly branching elastic tubes", J. Biophys, vol. 6, issue 1, 1966.

[73] M.A.Awal, S.S. Mostafa, M. Ahmad, "Performance Analysis of Savitzky-Golay Smoothing Filter Using ECG Signal", International Journal of Computer and Information Technology, vol. 01, no. 02, January 2011.

[74] M. A. Awal, S. S. Mostafa, M. Ahmad, "Simplified Mathematical Model For Generating ECG Signal and Fitting The Model using Nonlinear Least Square Technique", International Conference on Mechanical Engineering, December, 2011.

[75] M. A. Awal, S. S. Mostafa, M. Ahmad, "Quality Assessment of ECG Signal using Symlet Wavelet Transform", International Conference on Advances in Electrical Engineering, December, 2011.

[76] S. S. Mostafa, M. A. Awal, M. M. Islam, M. Ahmad, "Correlation of Heart-rate and Cardiac Cycle Duration under Different Body Positions and Breathing", International Conference on Advances in Electrical Engineering, December, 2011.

[77] M. A. Awal, S. S. Mostafa, M. Ahmad, M. A. Rashid, M. F.B. Abd Malek, "A Mathematical Model for Generating ECG Signal in Different Cardiac Dysrhythmias", accepted for publication in Medicina.

APPENDIX

APPENDIX I: Coefficient coiflet and symlet wavelet of order 3,4,5 used in the research.

a) Lowpass coefficient h_n for Coiflet wavelet. Highpass coefficient g_n can be calculated from h_n using eq.5.28.

h_n	Coif3	Coif4	Coif5
0	0.003793513	-0.0008923	0.000212081
1	0.007782596	-0.0016295	0.00035859
2	-0.023452696	0.00734617	-0.002178236
3	-0.065771911	0.01606894	-0.004159359
4	0.06112339	-0.0266823	0.010131118
5	0.405176902	-0.0812667	0.023408157
6	-0.793777223	0.05607731	-0.028168029
7	0.428483476	0.41530841	-0.091920011
8	0.071799822	-0.7822389	0.052043163
9	-0.082301927	0.43438606	0.421566207
10	-0.034555028	0.06662747	-0.774289604
11	0.015880545	-0.0962204	0.437991626
12	0.009007976	-0.0393344	0.062035964
13	-0.002574518	0.02508226	-0.105574209
14	-0.001117519	0.01521173	-0.041289209
15	0.000466217	-0.0056583	0.032683574
16	7.10e-05	-0.0037514	0.019761779
17	-3.46e-05	0.00126656	-0.009164231
18		0.00058902	-0.006764185
19		-0.00026	0.002433373
20		-6.23e-05	0.001662864
21		3.12e-05	-0.000638131
22		3.26e-06	-0.00030226
23		-1.78e-06	0.000140541
24			4.13e-05
25			-2.13e-05
26			-3.73e-06
27			2.06e-06
28			1.67e-07
29			-9.52e-08

b) Lowpass coefficient h_n for Symlet wavelet. Highpass coefficient g_n can be calculated from h_n using eq.5.28.

h_n	Sym3	Sym4	Sym5
0	-0.3326706	-0.032223	-0.01953888
1	0.8068915	-0.012604	-0.02110183
2	-0.4598775	0.0992195	0.17532809
3	-0.135011	0.2978578	0.01660211
4	0.0854413	-0.803739	-0.63397896
5	0.0352263	0.4976187	0.72340769
6		0.0296355	-0.19939753
7		-0.075766	-0.03913425
8			-0.02951949
9			0.02733307

Appendix II: Derivation of the T-function for the heart-arterial interaction model.

The basic computational unit is a segment of artery which is considered as a thin-walled uniform cylindrical tube having internal viscous, elastic and inertial properties with external coupling to the surrounding tissue producing a longitudinal constraint. This representation was previously used by [64], [65] to solve the Navier-Stokes equations for fluid flow in elastic tubes and apply the solution to pulsatile blood flow in arteries.

The wave propagation in the fluid-filled elastic tube is described [66]by,

$$\left.\begin{aligned} \frac{\partial q}{\partial t} + cZ_0 \frac{\partial p}{\partial x} = 0 \\ \frac{\partial q}{\partial t} + \frac{c}{Z_0} \frac{\partial q}{\partial x} = 0 \end{aligned}\right\} \tag{1}$$

where p and q are pressure and volumetric rate of flow in a tube respectively, and c is pulse wave velocity.

In Eq. 1, Z_0 is characteristic impedance defined as,

$$Z_0 = \frac{\rho c}{A} \tag{2}$$

where ρ is fluid density in a tube, and A is the cross sectional area of the tube.

Reflections are generated in a vascular system wherever there is a local change of impedance. Wave reflections in the tube have the effect of modifying the pressure and flow in the tube because the reflected waves combine with the forward traveling waves.

For the applied pressure $P_0 e^{i\omega t}$ at the tube entrance, the solution of Eq. 1 is,

$$\begin{aligned} p(x,t) &= p_f(x,t) + p_b(x,t) \\ &= P_0 e^{i\omega t - \gamma x} + \Gamma P_0 e^{i\omega t + \gamma(x-2z)} \end{aligned} \tag{3}$$

where p_f is forward traveling pressure wave, p_b is backward traveling pressure wave and γ is wave propagation constant defined as

$$\gamma = \frac{j\omega}{c} \tag{4}$$

The reflection constant Γ is given as

$$\Gamma = \frac{p_b(z,t)}{p_f(z,t)} \tag{5}$$

The solution for the flow of Eq. 1 is

$$\begin{aligned} p(x,t) &= q_f(x,t) + q_b(x,t) \\ &= Z_0\left(p_f(x,t) - p_b(x,t)\right) \end{aligned} \tag{6}$$

The concept of vascular impedance was borrowed from electrical engineering, and it is defined as

$$Z(x) = \frac{p(x,t)}{q(x,t)} = Z_0 \frac{p_f(x,t) + p_b(x,t)}{p_f(x,t) - p_b(x,t)} \tag{7}$$

From Eq. 3 and Eq. 7, the input impedance of tube ($x = 0$) is

$$Z_I = Z(0) = Z_0 \frac{1 + \Gamma e^{-2\gamma z}}{1 - \Gamma e^{-2\gamma z}} \tag{8}$$

According to Eq. 8, if there is no wave reflection, the input impedance is the characteristic impedance.

From Eq. 3 and Eq. 7, the terminal impedance of tube ($x = z$) is

$$Z_T = Z(z) = Z_0 \frac{1 + \Gamma}{1 - \Gamma} \tag{9}$$

The reflection coefficient Γ, determined from Eq.9 is

$$\Gamma = \frac{Z_T - Z_0}{Z_T + Z_0} \tag{10}$$

The pressure transfer function [67] is the pressure at the termination ($x = z$, called distal pressure, P_{distal}) to pressure at the origin ($x = 0$, called proximal pressure, $P_{proximal}$) is

$$T = \frac{p(z,t)}{p(0,t)} = \frac{P_{distal}}{P_{proximal}} = \frac{e^{-\gamma z} + \Gamma e^{-\gamma z}}{1 + \Gamma e^{-2\gamma z}} = \frac{(1+\Gamma)e^{-\gamma z}}{1 + \Gamma e^{-2\gamma z}} \tag{11}$$

The wave propagation constant γ and the characteristic impedance Z_0 can be derived by pulsatile blood flow theory [68]. Here we discuss a brief description.

Pulsatile Blood Flow in a Vascular Tube

Womersley Model

The blood vessels are fully constrained by adjacent muscles and other tissues. With this constraint in mind, [64] suggested the following model

$$q = \frac{A(-\frac{\partial p}{\partial x})}{j\omega\rho}(1 - F_{10}) \tag{12}$$

$$\text{Where } F_{10} = \frac{2J_1(\alpha j^{3/2})}{\alpha j^{3/2} J_0(\alpha j^{3/2})} \tag{13}$$

where J_o and J_1 are Bessel functions of the first kind, and order zero and one, respectively, and Womersley number, $\alpha = R_0\sqrt{\omega\rho/\mu}$. (14)

Vascular Wall

The arterial wall is known to behave as a viscoelastic material [69] which has the property of producing a phase difference between applied force and resulting displacement. This frequency dependent property is thus described by the dynamic Young's modulus E_d [69], expressed as

$$E_d = E + j\omega\eta_w \tag{15}$$

where η_w is the wall viscosity.

With respect to pulse wave propagation, the viscoelastic properties of the arterial wall are characterized by the tangent of the angle ~ representing the phase lead of pressure in relation to wall displacement. [70] , [71].

$$\theta = \tan^{-1}\left(\frac{\omega\eta_w}{E}\right) \tag{16}$$

Reference [72] derived an expression for the variation of θ with frequency as

$$\theta = \theta_0(1 - e^{-k\omega}) \tag{17}$$

where θ_0 is an asymptotic value and k was taken as 2.

Pulse Wave Velocity

The pulse wave velocity of inviscid fluid is defined by Moens-Korteweg equation as

$$c_{0=}\sqrt{\frac{E_s h}{2\rho R}} \tag{18}$$

Reference [64] modeled the coupling effect of fluid and wall on the wave propagation as

$$c' = c_0\sqrt{\frac{1 - F_{10}}{1 - \sigma^2}} \tag{19}$$

By use of the viscoelastic property of vascular wall, the equation of wave velocity becomes

$$c = c'e^{j\theta/2} \tag{20}$$

The equations for characteristic impedance and propagation constant of vascular tube is

$$Z_0 = \frac{\rho c_0}{\sqrt{1-\sigma^2}} \times (1 - F_{10})^{-1/2} \times \{\cos(\theta/2) + j\sin(\theta/2)\} \tag{21}$$

$$\gamma = \frac{\omega}{c_0} \times \frac{\sqrt{1-\sigma^2}}{\sqrt{1-F_{10}}} \times \{\cos(\theta/2) - j\sin(\theta/2)\}$$

$$\text{or, } \gamma = \frac{\omega}{c_o}\frac{\sqrt{1-\sigma^2}}{\sqrt{1-F_{10}}}e^{-j\theta/2} \tag{22}$$